

1 **Current, steady-state and historical weathering rates of base**  
2 **cations at two forest sites in northern and southern Sweden: A**  
3 **comparison of three methods**

4 Sophie Casetou-Gustafson<sup>1\*</sup>, Harald Grip<sup>2</sup>, Stephen Hillier<sup>3, 5</sup>, Sune Linder<sup>4</sup>, Bengt A.  
5 Olsson<sup>1</sup>, Magnus Simonsson<sup>5</sup> Johan Stendahl<sup>5</sup>

6  
7 <sup>1</sup>Department of Ecology, Swedish University of Agricultural Sciences, (SLU), P.O. Box 7044, SE-750 07  
8 Uppsala, Sweden. \*Present address: Norra Kyrkogatan 18A, SE-452 30 Strömstad, Sweden.

9 <sup>2</sup>Department of Forest Ecology and Management, SLU, SE-901 83 Umeå, Sweden. Present address: Stjernströms  
10 väg 5, SE-129 35 Hägersten, Sweden

11 <sup>3</sup>The James Hutton Institute, Craigiebuckler, Aberdeen AB15 8QH, United Kingdom

12 <sup>4</sup>Southern Swedish Forest Research Centre, SLU, P.O. Box 49, SE-230 53 Alnarp, Sweden

13 <sup>5</sup>Department of Soil and Environment, SLU, P.O. Box 7014, SE-750 07 Uppsala, Sweden

14  
15 *Correspondence to:* Sophie Casetou-Gustafson (Sophie.Casetou@slu.se)

16  
17  
18  
19  
20  
21  
22  
23  
24

25  
26

27 **Abstract**

28         Reliable and accurate methods for estimating soil mineral weathering rates are required tools in  
29 evaluating the sustainability of increased harvesting of forest biomass and assessments of critical loads of  
30 acidity. A variety of methods that differ in concept, temporal and spatial scale and data requirements are  
31 available for measuring weathering rates. In this study, causes of discrepancies in weathering rates between  
32 methods were analyzed and were classified as being either conceptual (inevitable) or random. The release rates  
33 of base cations (BC; Ca, Mg, K, Na) by weathering were estimated in podsolised glacial tills at two experimental  
34 forest sites, Asa and Flakaliden, in southern and northern Sweden, respectively. Three different methods were  
35 used: (i) historical weathering since deglaciation estimated by the depletion method, using Zr as assumed inert  
36 reference; (ii) steady-state weathering rate estimated with the PROFILE model, based on quantitative analysis of  
37 soil mineralogy; and (iii) BC budget at stand scale, using measured deposition, leaching and changes in base  
38 cation stocks in biomass and soil over a period of 12 years. In the 0–50 cm soil horizon historical weathering of  
39 BC were 10.6 and 34.1 mmol<sub>c</sub> m<sup>-2</sup> yr<sup>-1</sup> at Asa and Flakaliden, respectively. Corresponding values of PROFILE  
40 weathering rates were 37.1 and 42.7 mmol<sub>c</sub> m<sup>-2</sup> yr<sup>-1</sup>. The PROFILE results indicated that steady-state weathering  
41 rate increased with soil depth as a function of exposed mineral surface area, reaching a maximum rate at 80 cm  
42 (Asa) and 60 cm (Flakaliden). In contrast, the depletion method indicated that the largest postglacial losses were  
43 in upper soil horizons, particularly at Flakaliden.

44         With the exception of Mg and Ca in shallow soil horizons, PROFILE produced higher weathering rates  
45 than the depletion method, particularly of K and Na in deeper soil horizons. The lower weathering rates of the  
46 depletion method was partly explained by natural and anthropogenic variability in Zr gradients. The base cation  
47 budget approach produced significantly higher weathering rates of BC; 134.6 mmol<sub>c</sub> m<sup>-2</sup> yr<sup>-1</sup> at Asa and 73.2  
48 mmol<sub>c</sub> m<sup>-2</sup> yr<sup>-1</sup> at Flakaliden, due to high rates rates estimated for the nutrient elements Ca, Mg and K, whereas  
49 weathering rates were lower and similar to the depletion method (6.6 and 2.2 mmol<sub>c</sub> m<sup>-2</sup> yr<sup>-1</sup> at Asa and  
50 Flakaliden). The large discrepancy in weathering rates for Ca, Mg and K between the base cation budget  
51 approach and the other methods suggest additional sources for tree uptake in the soil not captured by  
52 measurements.

53

54 **Keywords.** Weathering; minerals; soil horizons; nutrient mass-balance; *Picea abies*; PROFILE model;  
55 depletion; base cation budget approach

56

57

58

59

60

61

62 **Definitions and abbreviations**

63 Mineralogy = The identity and stoichiometry of minerals present in a certain geographical unit, a particular site  
64 (*site-specific mineralogy*) or a larger geographical province (*regional mineralogy*)

65 Quantitative mineralogy or mineral composition = Quantitative information (wt.%) on the abundance of specific  
66 minerals in the soil.

67 Weathering rate = Weathering of a mineral resulting in release of base cations per unit area per unit time.

68

69  $W_{\text{depletion}}$  = Historical weathering rate based on calculation of loss of mobile elements since last deglaciation

70  $W_{\text{profile}}$  = Steady-state weathering rate estimated using the PROFILE model

71  $W_{\text{budget}}$  = Current weathering rate based on base cation budget calculations

72

73

74

## 75 **1. Introduction**

76 Silicate weathering is the major long-term source of base cations in forest ecosystems (Sverdrup and Warfvinge,  
77 1988) and is therefore crucial for sustainable plant production and for proton consumption, counteracting soil  
78 and water acidification (Nilsson et al., 1982; Hedin et al., 1994; Likens et al., 1998; Bailey et al., 2003). These  
79 effects of weathering are important in areas where in the past high sulphur (S) deposition has caused severe  
80 acidification of forest soils and waters (Reuss and Johnson, 1986), for example in southern Scandinavia,  
81 northeastern USA and southeastern Canada, regions where felsic igneous bedrock and less readily weatherable  
82 soils are abundant (Likens and Bormann, 1974; Nilsson and Tyler, 1995). To aid the multi-lateral negotiations  
83 on reducing emissions of acidifying air pollution, the effect-based concept of critical loads of acidity was  
84 developed in the late 1980s (Lidskog and Sundqvist, 2002). One advantage of the concept was that the critical  
85 loads could be calculated and mapped for different regions at various scales. Because weathering is a key  
86 component in estimates of critical loads, reliable applications of the critical load concept required that  
87 weathering rates could be estimated with sufficient accuracy at regional scale (Sverdrup and de Vries, 1994).

88  
89 By 1990 in most European countries, the trend of increasing S emissions since the 1950s started to abate  
90 (Grennfelt and Hov, 2005) with a simultaneous decrease in atmospheric deposition of base cations (Hedin et al.  
91 1994). In Sweden, forest growth has at the same time gradually become a relatively more important source to  
92 soil acidity (Iwald et al., 2013). Besides the reduction in S deposition, this change has partly been driven by  
93 increased use of logging residues for energy production (i.e. whole-tree harvesting), and probably also by a  
94 general higher forest production over recent decades in Sweden (Binkley and Högborg 2016). Soil acidification  
95 by forest growth is principally caused by accumulation of base cations in tree biomass in excess of anion uptake  
96 (Nilsson et al., 1982). The return of base cations in remaining biomass and residues following harvesting  
97 determines to what extent the acid load can be neutralised. The soil acidification effect of whole-tree compared  
98 to stem-only harvesting has been demonstrated in long-term field experiments (Olsson et al., 1996; Zetterberg et  
99 al., 2013). The combined effects can therefore impede recovery from acidification and place increasing demands  
100 on nutrient supply.

101  
102 The sustainability of increased harvest intensity of forest biomass has been questioned and analysed in many  
103 studies from various viewpoints and criteria with focus on Europe and North America (e.g. Boyle et al., 1973;  
104 Paré et al., 2002; Thiffault et al., 2011, Achat et al. 2015; De Jong et al., 2017; Ranius et al., 2018), where the  
105 role of weathering in maintaining base cation balance being one criterion. The impact of increased use of logging  
106 residues on base cation balances in Swedish forest soils has been examined in several previous studies (Sverdrup  
107 and Rosén, 1998; Akselsson et al., 2007). A regional-scale study on Swedish forest soils found that, in parts of  
108 Sweden, base cation losses can occur at rates that lead to very low base saturation of the soils, possibly leading  
109 to negative effects on e.g. soil fertility and runoff water quality within just one forest rotation (Akselsson et al.,  
110 2007). In their study, base cation depletion in the soil was found to be more common after whole-tree harvesting  
111 than stem-only harvesting, especially for Norway spruce, with deficits being more common in southern than in  
112 northern (boreal) Sweden.

113

114 In regional assessments of the sustainability of different harvesting regimes, the estimated weathering rate has a  
115 strong influence on the base cation balance. Klaminder et al. (2011) found that different approaches to estimating  
116 weathering rates for a forested catchment in northern Sweden yielded results that differed substantially, and that  
117 uncertainties in the methods had a great influence on the predicted sustainability of different harvesting  
118 practices. Futter et al. (2012) compiled weathering rates estimated at 82 sites on three continents, using different  
119 methods, and found both large between-site as well as within-site differences in the values. Differences in input  
120 data can be attributed to different time scales used when acquiring different input data, challenges determining  
121 accurate mineralogical compositions and the use of field data compared with laboratory data (Van der Salm,  
122 2001; Futter et al., 2012). Thus, they recommend that at least three different approaches be applied per study site  
123 to evaluate the precision in weathering estimates.

124  
125 Different approaches to estimate weathering rates are likely to produce different estimates due to their  
126 conceptual differences, but additional sources to discrepancies of more random nature will also appear. The  
127 latter may be due to e.g. misfits in spatial scales, measurement errors or uncertainties in model parametrisation.  
128 A number of studies comparing different approaches to estimate weathering rates have been published (e.g.  
129 Kolka et al., 1996; Sverdrup et al, 1998; Van der Salm et al., 2001; Ouimet and Dechesne, 2005; Whitfield et al.,  
130 2006, 2011; Koseva et al., 2010; Klaminder et al., 2011; Stendahl et al., 2013; Futter et al., 2012; Augustin et al.,  
131 2016) such that additional studies on this issue may seem redundant. However, several of these comparison  
132 studies can be criticized for poor harmonisation with respect to the spatial scale, or that nutrient uptake in  
133 biomass and soil change have been neglected, or poorly quantified in approaches where these processes are  
134 relevant for the estimates. Poor harmonisation makes it difficult to separate conceptual from random sources of  
135 discrepancies. We therefore see a need for improved comparisons, performed with a spatially constrained and  
136 refined harmonisation in the sense of Futter et al. (2012), and combined with a focus on forest soils, tree  
137 nutrition and growth. Starting from the viewpoint that no method provides the 'true' estimate of weathering, and  
138 acknowledging that different approaches are conceptually different and use different input data, in the present  
139 paper we examined three approaches in the present paper: (1) 'historical weathering' based on geochemical  
140 investigation of the soil profile, (2) modelled present weathering rate and (3) present weathering rate based on  
141 cation balances at the ecosystem level.

142  
143 The choice of methods was primarily based on the fact that rates of weathering may (do) vary over time  
144 (Klaminder et al., 2011; Stendahl et al., 2013). The average weathering under long-term environmental change,  
145 i.e. 'historical weathering', is thus different from the weathering potential under present-day environmental  
146 conditions, i.e. 'present-day weathering', which is why we need to be able to consider historical weathering  
147 when assessing current/present-day weathering rates. Moreover, present-day weathering rates estimated by  
148 models based on the steady-state concept, which lacks the dimension of time, may differ from dynamic estimates  
149 of weathering rates derived from measured base cation budgets. These three different concepts of estimating  
150 weathering cannot be covered by a single method (Klaminder et al., 2011; Futter et al., 2012). Indeed,  
151 weathering estimates based on these concepts have often differed grossly from pedon to catchment scale,  
152 whereas truly harmonised comparisons of methods require that methods are tested uniformly at the same spatial  
153 scale. This spatial scale can be the pedon, which also contains the major part of the mineral nutrient sources in

154 the soil available for forest growth. To our knowledge, Kolka et al. (1996) is the only study to have previously  
155 used this multiple approach.

156

157 The first approach, the depletion method, makes use of soil profile based mass balances (Chadwick et al., 1990;  
158 Brimhall et al., 1991) to estimate total base cation losses in the soil above a reference soil depth. An element in a  
159 weathering-resistant mineral is used as a standard, most commonly zirconium (Zr, present in e.g. zircon) or  
160 titanium (Ti, present in e.g. rutile) (Sudom and St. Arnaud, 1971; Harden, 1987; Chadwick et al., 1990; Bain et  
161 al., 1994), due to their resistance to weathering at low temperatures (Schützel et al., 1963). To yield an annual  
162 average weathering rate ( $\text{mmol}_e \text{ m}^{-2}$ ), calculated element losses are commonly divided by an estimated soil age.  
163 In Nordic glacial tills situated above the marine limit, soil age is conventionally considered to be the number of  
164 years lapsed since the site of interest was finally deglaciated at the end of the Weichselian. Because the rate of  
165 weathering may vary over time (Klaminder et al., 2011; Stendahl et al., 2013), the average ‘historical  
166 weathering’ rate may differ from the present-day weathering rate.

167

168 The second approach commonly involves the process-based PROFILE model, which has been used widely as a  
169 tool to estimate critical loads of acidity in the Nordic countries (e.g. Sverdrup et al., 1992) and North America  
170 (Whitfield and Watmough, 2012; Phelan et al., 2014). In PROFILE, release rates of base cations are estimated  
171 based on built in assessments of the the dissolution kinetics of a user-defined set of minerals present in the soil,  
172 and the physical and chemical conditions that drive the dissolution of those minerals. Because it is a mechanistic  
173 model, its strength is its transparency, while its main weakness is the difficulty in setting values of model  
174 parameters and input variables to which it may have high sensitivity. Akselsson et al. (2019) concluded that the  
175 most important way to reduce uncertainties in modelled weathering rates is to reduce input data uncertainties,  
176 e.g. regarding soil texture, although there is still a need to improve process descriptions of e.g. biological  
177 weathering and weathering brakes (e.g. Erlandsson Lampa et al., this issue). The sensitivity of PROFILE to  
178 variations in soil physical parameters (e.g. soil texture, soil bulk density) and mineral composition was discussed  
179 by Jönsson et al. (1995) and Hodson et al. (1996). The importance of the ability to determine the precise identity  
180 and quantity of the minerals was analysed by Casetou-Gustafson et al. (2019). They (ibid.) also suggested that  
181 the dissolution kinetics of minerals used in the PROFILE model should be revised and the uncertainties assessed  
182 to improve the accuracy in model predictions.

183

184 The third approach to estimating weathering rate is the balanced base cation budget approach. This method has  
185 been applied to estimate current weathering rates at various temporal and spatial scales, mostly the catchment  
186 scale (Velbel, 1985; Likens et al., 1998). In one way of using the approach, mean weathering rates of individual  
187 minerals can be estimated at the catchment scale based on data for the mineralogical composition of soils along  
188 with element inputs in deposition and outputs in stream water and biomass uptake (e.g. Garrels and Mackenzie,  
189 1967; Velbel 1985, Velbel and Price, 2007). Others have estimated weathering as an unknown source from the  
190 missing balance between known sources (deposition, soil depletion) and known sinks (uptake, leaching, increase  
191 in soil BC stocks) (e.g. Sverdrup et al. 1998; Simonsson et al., 2015). The method requires measurements of  
192 known fluxes within a system with defined boundaries. The high data demand restricts the application of the  
193 base cation budget approach to a limited number of sites, essentially catchments with long-term monitoring of

194 fluxes and well-defined boundaries. However, even then estimated weathering rates may suffer from large  
195 uncertainties, as errors in the sinks and sources accumulate in the mass balance equation (Simonsson et al.,  
196 2015). Furthermore, the base cation budget approach has mostly been applied under conditions where  
197 accumulation in biomass were not directly measured but estimated to be small, or base cation stocks in the soil  
198 were assumed to be at steady-state (e.g. Kolka et al., 1996; Sverdrup et al., 1998; Whitfield et al., 2006).  
199 However, the nutrient demand is particularly large during the aggrading phase of a stand development where the  
200 foliage biomass is increasing rapidly. Hence, due to difficulties in application of the budget method to regional  
201 scale, the PROFILE model and the depletion method are the most commonly used methods in Sweden to  
202 estimate weathering rates.

203

204 The principal aim of this study was to analyse the causes of discrepancies in estimations of weathering rates,  
205 with focus on conceptual versus random sources of discrepancies, between the depletion method, the PROFILE  
206 model and the balanced base cation budget approach. To accomplish this aim, the specific aims were to (1)  
207 perform a spatially harmonized comparison, *sensu* Futter et al. (2012) of the three approaches for a set of test  
208 criteria, and (2) to place weathering in the context of other base cation fluxes in aggrading Norway spruce  
209 forests, in particular the uptake in forest biomass. The base cation budgets were estimated at the period of stand  
210 development when nutrient demand was expected to peak. In combination with access to highly accurate data on  
211 biomass production, these conditions also provided opportunities to relate weathering to base cation  
212 accumulation in biomass at high nutrient uptake rates, and possible simultaneous depletions of extractable base  
213 cation stocks in the soil. Furthermore, input data to PROFILE were characterised by high quality quantitative  
214 mineralogical data, measured directly by quantitative X-ray powder diffraction (XRPD), as previously discussed  
215 by Casetou-Gustafson et al. (2018). Discrepancies between the PROFILE model and the depletion method were  
216 analysed by testing the sensitivity of PROFILE to changes in soil physical or mineralogical composition, and by  
217 calculating the hypothetical time needed for PROFILE weathering rates to accomplish the element loss observed  
218 with the depletion method.

219

220 Three test criteria were used to examine the outputs of the depletion method and PROFILE model: (1) similarity  
221 in weathering estimates for the 0-50 cm soil profile; (2) similarity in depth gradients in weathering for the 0-100  
222 cm soil profile; and (3) similarity in ranking order of the base cations released.

## 223 **2. Materials and methods**

### 224 **2.1 Study sites**

225 Two forest sites planted with Norway spruce (*Picea abies* (L.) Karst) were chosen for the study, Flakaliden in  
226 northern Sweden (64°07'N, 19°27'E) and Asa in southern Sweden (57°08'N, 14°45'E), because they have been  
227 used for long-term experimental studies on the effects of climate and nutrient and water supply on tree growth  
228 and element cycling (Linder, 1995; Bergh et al., 1999; Ryan, 2013) (Fig. 1).

229

230 The experiment at Flakaliden was established in 1986 in a 23-year-old Norway spruce stand, planted in 1963  
231 with four-year-old seedlings of local provenance after prescribed burning and soil scarification (Bergh et al.,  
232 1999). The experiment at Asa was established one year later (1987), in a 12-year-old Norway spruce stand

233 planted in 1975 with two-year-old seedlings after clear-felling and soil scarification. The experimental design  
234 was similar at both sites and included control, irrigation and two nutrient optimisation treatments (Bergh et al.,  
235 1999). All treatments were replicated in 50 m × 50 m plots, arranged in a randomised block design. Only two of  
236 the four treatments were used in the present study; the control (C) and plots receiving an annual dose of an  
237 optimised mix of solid fertiliser (F), which among other elements per year contained about 10 kg ha<sup>-1</sup> Ca, 8 kg  
238 ha<sup>-1</sup> Mg and 45 kg ha<sup>-1</sup> K (Linder, 1995).

239  
240 Flakaliden is located in the central boreal sub-zone with a harsh climate, with long cool days in summer and  
241 short cold days in winter. Mean annual temperature for the period 1990-2009 was 2.5 °C, and mean monthly  
242 temperature varied from -7.5 °C in February to 14.5 °C in July. Mean annual precipitation in the period was  
243 ~650 mm, with approximately one-third falling as snow, which usually covers the frozen ground from mid-  
244 October to early May. Mean length of the growing season (daily mean temperature ≥ 5 °C) was 148 days, but  
245 with large between-year variations (cf. Table 1 in Sigurdsson et al., 2013).

246  
247 Asa is located in the hemi-boreal zone, where the climate is milder than at Flakaliden, which is reflected in a  
248 longer growing season (193 days). Mean annual temperature (1990-2009) was 6.3 °C, mean monthly  
249 temperature varied from -1.9 °C in February to 16.0 °C in July and mean annual precipitation was ~750 mm.  
250 The soil is periodically frozen in winter. The difference in climate is reflected in differences in site productivity,  
251 which broadly follows climate gradients in Sweden (Bergh et al., 2005).

252  
253 The soils at Asa and Flakaliden differ in age due to differences in the time since deglaciation (Table 1), from  
254 approximately 14,300 years at Asa and 10,150 years at Flakaliden (estimated from Fredén, 2009). The soil type  
255 at both sites is an Udic Spodosol, with a mor humus horizon overlying glacial till derived from felsic bedrock.  
256 The soil texture is classified as sandy loam. The transition between the B- and C-horizons is mostly located at 50  
257 cm depth at Flakaliden and 50-60 cm depth at Asa. The natural ground vegetation at Flakaliden is dominated by  
258 *Vaccinium myrtillus* (L.) and *V. vitis-idaea* (L.) dwarf-shrubs, lichens and mosses (Kellner, 1993; Strengbom et  
259 al., 2011). The ground vegetation at Asa is dominated by *Deschampsia flexuosa*, (L.) and mosses (Strengbom et  
260 al., 2011; Hedwall et al., 2013).

## 261 2.2. Soil sampling and analyses of geochemistry and mineralogy

262 A detailed description of soil sampling, geochemical analyses and determination of mineralogy can be found in  
263 Casetou-Gustafson et al. (2018). The procedures are summarised below. Sampling was performed in untreated  
264 control plots (K1 and K4 at Asa and 10B and 14B at Flakaliden) and fertilised (F) plots (F3, F4 at Asa and 15A  
265 and 11B at Flakaliden) in October 2013 (Flakaliden) and March 2014 (Asa), in the border zone of four plots at  
266 each site. One intact soil core per plot at Flakaliden and in plot K1 at Asa was extracted using a rotary drill (17  
267 cm inner diameter). In plots K4, F3 and F4 at Asa, soil samples were instead taken from 1 m deep manually dug  
268 soil pits, due to inaccessible terrain for the rotary drill machinery. Maximum soil depth was shallower at  
269 Flakaliden (70-90 cm) than at Asa (90-100 cm). The volume of stones and boulders was determined for each plot  
270 at the two study sites using the penetration method described by Viro (1952) to a maximum depth of 30 cm and



271 by applying the fitted function described by Stendahl et al. (2009). Mean stone and bolder content was higher at  
272 Flakaliden (39%vol.) than at Asa (28%vol.).

273

274 Soil samples were taken from each 10-cm soil horizon. Prior to chemical analysis, these samples were dried at  
275 30-40 °C and sieved to <2 mm. Analysis of particle size distribution was performed by wet sieving and  
276 sedimentation (pipette method) in accordance with ISO 11277. Geochemical analyses were conducted by ALS  
277 Scandinavia AB and comprised inductively coupled plasma-mass spectrometry (ICP-MS) on HNO<sub>3</sub> extracts of  
278 fused samples that were milled and ignited (1000 °C) prior to fusion with LiBO<sub>2</sub>.

279

280 Quantitative soil mineralogy was determined with the X-ray powder diffraction (XRPD) technique (Hillier 1999,  
281 2003). Samples for measurement of XRPD patterns were prepared by spray drying slurries of soil samples (<2  
282 mm) micronised in ethanol. A full pattern fitting approach was used for quantitative mineralogical analysis of  
283 the diffraction data (Omotoso et al., 2006). This fitting process involved the modelling of the measured  
284 diffraction pattern as a weighted sum of previously measured and verified standard reference patterns of the  
285 identified mineral components. The determination of chemical compositions of various minerals present in the  
286 soils was conducted by electron microprobe analysis (EMPA) of mineral grains subsampled from the sifted (< 2  
287 mm) soil samples. Mineralogical composition of the soils is given in the Supplement (Table S1).

## 288 **2.3 Historical weathering determined with the depletion method**

### 289 **2.3.1 Method description**

290 The depletion method (Table 2), as defined by Marshall and Haseman (1943) and Brimhall et al. (1991),  
291 estimates the accumulated mass loss since soil formation (last deglaciation for our sites) as a function of loss of a  
292 mobile (weatherable) element and enrichment of an immobile (weathering resistant) element according to the  
293 following general function introduced by Olsson and Melkerud (1989) and based on the same theories as the  
294 mass transfer function described in Brimhall et al. (1991):

$$295 \quad W_{\text{depletion},i} = \frac{d \cdot \rho}{100} \cdot \frac{X_c \cdot Zr_{w,i}}{Zr_c} - X_{w,i} \quad \text{Eq. 1}$$

296 where  $W$  denotes loss of the  $i$ th element ( $\text{g m}^{-2}$ ),  $X$  denotes mobile element concentrations (‰),  $Zr$  denotes  
297 immobile element concentrations (‰),  $w$  and  $c$  denote a weathered soil horizon and the assumed unweathered  
298 reference horizon, respectively,  $d$  is horizon thickness (m), and  $\rho$  is bulk density ( $\text{g m}^{-3}$ ). Zirconium is  
299 commonly used as the immobile element due to the inert nature of the mineral zircon ( $\text{ZrSiO}_4$ ), although Ti is  
300 sometimes used due to the resistance of the Ti-containing minerals anatase and rutile ( $\text{TiO}_2$ ) to weathering  
301 (Olsson and Melkerud, 1989). The unweathered reference horizon is located in the C horizon, and has X to Zr  
302 ratios that are assumed to represent pristine conditions of the presently weathered horizons above it. In the  
303 weathered horizons, X to Zr ratios are smaller; that is, Zr is enriched compared with the mobile elements (i.e. the  
304 base cations). The method is based on the assumptions that Zr, hosted in zircon, was uniformly distributed  
305 throughout the soil profile at the time of deglaciation, that weathering only occurs above the reference horizon  
306 and that zircon does not weather. The latter implies that Zr concentrations and Zr/base cation ratios are constant  
307 below the reference horizon. The reference depths for different base cations compared with Zr, which were used  
308 as the depths of immobile element concentrations, are shown in Table 3. The Zr/base cation ratio (Fig. S1) was

309 used to help select the reference soil horizon as it highlights heterogeneities in parent material with depth. In  
310 cases of heterogeneities in the profile, the reference horizon was chosen above this heterogeneity. This choice  
311 was precluded for soil profile 11B, where Zr concentrations and Zr/base cation ratios peaked directly below the  
312 B-horizon (i.e. at 50-60 cm).

### 313 2.3.2. Application

314 Prior to calculating base cation weathering rates with the depletion method, fractional volume change  $V_p$  was  
315 calculated according to White et al. (1996) in order to assess if there were any large volume changes (collapse)  
316 in the mineral soil with implications for which depth the weathering should be calculated to. Similar to White et  
317 al. (1996), it was assumed that values close to zero indicate no volumetric change, which was the case below 30-  
318 40 cm of soil depth at both sites (Table S2). The homogeneity of the parent material was also evaluated (Fig. 2)  
319 using the criterion that the ratio of Ti to Zr should be more or less constant with depth in an originally  
320 homogeneous material. Use of the ratio of two immobile elements to establish uniformity of parent material has  
321 been suggested previously (Sudom and St. Arnaud, 1971; Starr et al., 2014). The homogeneity criterion was not  
322 met using Zr in plot K1 at Asa (i.e. the Zr concentrations decreased towards the soil surface; Fig. 2); here Ti was  
323 used as the immobile element instead. Furthermore, the plots 15A and 11B at Flakaliden had to be eliminated  
324 from the calculations, because relatively large variability in both the Zr and Ti gradients was observed. These  
325 large heterogeneities led to an overall gain of base cations in the rooting zone, which is opposite to what would  
326 be expected (i.e. that losses and gains can occur at specific soil depths due to eluviation and illuviation processes  
327 in podzolic soils). For this reason, soil profiles 15A and 11B were eliminated from further consideration in  
328 calculations of historical weathering rates using the depletion method. Thus, apart from heterogeneities,  
329 transportation processes (eluviation and illuviation) and/or erratic Zr or Ti gradients could lead to “negative”  
330 weathering, i.e. leading to a calculated relative accumulation of elements. Such negative values were not  
331 considered in the calculation of historical weathering losses.

332  
333 Bulk density was estimated for each soil horizon except in some plots where density measurements could not be  
334 made below a certain soil depth. Bulk density in these cases was estimated using an exponential model for total  
335 organic carbon (TOC) and bulk density (BD,  $\text{g cm}^{-3}$ ) based on our own data. For Asa (soil horizons F3: 70-90  
336 cm; F4: 0-10, 30-40, 50-60, 60-70, 70-80, 80-90, 90-100 cm; and K4: 70-80, 80-90, 90-100 cm), the following  
337 function was used:

$$338 \quad \rho = 1.3 e^{-0.1 x} \quad \text{Eq. 2}$$

339 where  $x$  is TOC content (% of dry matter). For Flakaliden (soil horizons 14B: 80-90cm; 10B: 60-70 cm; and  
340 11B: 40-70 cm), the function used was:

$$341 \quad \rho = 1.8 e^{-0.2 x} \quad \text{Eq. 3}$$

### 342 2.4.1 The PROFILE model

#### 343 2.4.1 Model description

344 The steady state weathering of soil profiles was estimated using the biogeochemical PROFILE model (Table 2),  
345 where weathering of the  $i$ th base cation ( $W_{\text{profile}, i}$ ) is described by long-term mineral dissolution kinetics at the

346 interface of wetted mineral surfaces and the soil solution. PROFILE is a multilayer model, where parameters are  
347 specified for each soil layer based on field measurements and estimation methods (Warfvinge and Sverdrup,  
348 1995).

#### 349 **2.4.2 PROFILE parameter estimation**

350 A detailed description of the application of the PROFILE model to the soils and sites in the present study can be  
351 found in Casetou-Gustafson et al. (2019). The parameters used are listed in Table 4a, 4b.

352

353 Exposed mineral surface areas were estimated from soil bulk density and texture data using the algorithm  
354 specified in Warfvinge and Sverdrup (1995). Volumetric soil water content for each soil profile in Flakaliden  
355 and Asa was estimated to be  $0.25 \text{ m}^3 \text{ m}^{-3}$  according to the moisture classification scheme described in Warfvinge  
356 and Sverdrup (1995) (Table S3).

357

358 The aluminium (Al) solubility coefficient, a soil chemical parameter needed for solution equilibrium reactions,  
359 was defined as  $\log\{\text{Al}^{3+}\}+3\text{pH}$ . It was estimated by applying a function developed from previously published  
360 data (Simonsson and Berggren, 1998) and existing total carbon and oxalate-extractable Al measurements for the  
361 sites (Casetou-Gustafson et al., 2018) (Table S3). For partial  $\text{CO}_2$  pressure in the soil, the default value of  
362 Warfvinge and Sverdrup (1995) was used. Data on measured dissolved organic carbon (DOC) in the soil  
363 solution at 50 cm depth were available for plots K4 and K1 at Asa and plots 10B and 14B at Flakaliden, and  
364 these values were also applied for deeper soil horizons. Shallower horizons (0-50 cm) were characterised by  
365 higher DOC values, based on previous findings (Fröberg et al., 2006, 2013) and the DOC classification scheme  
366 in Warfvinge and Sverdrup (1995) (Table S3).

367

368 Site-specific parameters used were evapotranspiration, temperature, atmospheric deposition, precipitation, runoff  
369 and nutrient uptake in biomass (Table 4a). Mean evapotranspiration per site was estimated from mean annual  
370 precipitation and runoff data, using a general water balance equation.

371

372 Total deposition was calculated using deposition data from two sites of the Swedish ICP Integrated Monitoring  
373 catchments, Aneboda (for Asa) and Gammtratten (for Flakaliden) (Löfgren et al., 2011). Na was used as a tracer  
374 ion in order to distinguish canopy exchange from dry deposition for Ca, Mg and K. Dry deposition for Na and Cl  
375 was calculated as the difference between wet and throughfall deposition. As outlined in Zetterberg et al. (2016),  
376 wet deposition for all elements was calculated by correcting bulk deposition for dry deposition using wet-only to  
377 bulk deposition ratio. Wet deposition was estimated based on the contribution of dry deposition to bulk  
378 deposition, both for base cations and anions, using dry deposition factors from Karlsson et al. (2011, 2013).  
379 Finally, total deposition for all elements was calculated from the sum of dry and wet deposition.

380

381 Net base cation and nitrogen uptake in aboveground tree biomass (i.e. bark, stemwood, living and dead branches,  
382 needles) was estimated as mean accumulation rate over a 100-year rotation period in Flakaliden and a 73-year  
383 rotation period in Asa. These calculations were based on Heureka simulations using the StandWise application

384 (Wikström et al., 2011) for biomass estimates, in combination with measured nutrient concentrations in  
385 aboveground biomass as described in section 2.5.4 below (Linder, unpubl. data).

### 386 **2.4.3 PROFILE sensitivity analysis**

387 The sensitivity of PROFILE to changes in soil physical and mineralogical input was analysed, to test to what  
388 extent the depth gradients of weathering rates as predicted by PROFILE were affected primarily by soil physical  
389 properties or by soil mineralogy. Independent PROFILE runs were performed, after replacing horizon-specific  
390 input values with soil profile average values regarding either (1) soil bulk density and specific exposed mineral  
391 surface area ('homogenous soil physics'), or (2) soil mineral percentages ('homogenous mineralogy'), or (3)  
392 both ('homogenous soil physics and mineralogy'). In each scenario, the squared deviation in weathering rate was  
393 calculated for each base cation and horizon, compared to the normal simulation based on horizon-specific inputs  
394 for soil physics and soil mineralogy. The sum of squares over base cations and horizons was used as a measure  
395 of the overall error caused by the 'homogenous' input data. The ratios of sum of squares, of scenario (1) over (3)  
396 and of scenario (2) over (3), was used to estimate the percent contribution of soil physics and soil mineralogy,  
397 respectively, to the overall weathering gradients in the soil profile.

## 398 **2.5 The base cation budget approach**

### 399 **2.5.1. General concepts of the base cation budget approach**

400 The average weathering rate of the  $i$ th base cation according to base cation budget,  $W_{\text{budget}, i}$ , over a period of  
401 time can be estimated with base cation budgets (Table 2) using the base cation budget approach, which assumes  
402 that total deposition ( $\square\square\square$ ) and weathering are the major sources of mobile and plant-available base cations in  
403 the soil, and that leaching ( $\square\square$ ) and accumulation of base cations in biomass ( $\Delta\square\square$ ) are the major sinks. A  
404 change in the extractable soil stocks of base cations over time ( $\Delta\square\square$ ) is considered as a sink if stocks have  
405 increased, or as a source if stocks have been depleted (Simonsson et al., 2015). Each of these terms is measured  
406 independently over a specific period of time. Hence,

$$407 \quad W_{\text{budget}, i} = L_i + \Delta B_i + \Delta S_i - TD_i \quad \text{Eq. 4}$$

### 408 **2.5.2 Atmospheric deposition, $TD_i$**

409 The same estimates of total atmospheric deposition as used in parameter setting of the PROFILE model (section  
410 2.4.2) were used in the base cation budget, Eq. (4).

### 411 **2.5.3. Changes in exchangeable soil pools, $\Delta S_i$**

412 Changes in extractable base cation stocks in the soil were calculated from the difference between two soil  
413 samplings, performed in 1986 and 1998 at Flakaliden, and in 1988 and 2004 at Asa. The organic horizon was  
414 sampled with a 5.6 cm diameter corer, whereas a 2.5 cm diameter corer was used to sample 10 cm sections to 40  
415 cm depth in the mineral soil. For each plot and horizon, 25 cores were combined into one sample.

416

417 Exchangeable base cation content in the soil (<2 mm) for all Flakaliden samples and in Asa for samples from  
418 1988 was determined by extraction of dry samples with 1 M  $\text{NH}_4\text{Cl}$  using a percolation method, where 2.5 g of

419 sample was leached with 100 mL of extractant at a rate of 20 mL h<sup>-1</sup>. The base cations were analysed by atomic  
420 absorption spectrophotometry (AAS). For the Asa samples from 2004, batch extraction was performed using the  
421 same extractant, and the base cations were determined with ICP. A separate test was made to compare the yield  
422 of the percolation and batch extraction methods. No consistent difference between the methods was observed.

423

424 The amount of fine soil (<2 mm) per unit area was calculated from the volume of fine earth (<2 mm) in the soil  
425 profiles and the average bulk density of the soil in the 0-10, 10-20 and 20-40 cm horizons. Bulk density and  
426 volume proportion of stoniness at Flakaliden were determined from samplings in 1986 in 20 soil profiles (0.5 m  
427 × 0.5 m and about 0.5 m deep) outside plots. At Asa, stoniness was determined with the penetration method of  
428 Stendahl et al. (2009) and the bulk density of soil <2 mm was calculated using a pedotransfer function that  
429 included soil depth and measured carbon concentrations as variables.

#### 430 **2.5.4 Net uptake in biomass, $\Delta B_i$**

431 Accumulation of base cations in tree biomass, i.e. net uptake of base cations, was calculated as a mean value of  
432 control plots over the period 1989-2003, based on increments in aboveground biomass at Asa and Flakaliden for  
433 this period and on the concentrations of elements in different tree parts. The increment in aboveground biomass  
434 was based on measurements of stem diameter at breast height (DBH) of all individual trees in the plots, and  
435 applying DBH data to allometric functions developed for Norway spruce at the sites (Albaugh et al., 2009,  
436 2012). The allometric functions were based on destructive samplings (1987 - 2003) of 93 and 180 trees at Asa  
437 and Flakaliden respectively. The increment in belowground biomass was estimated from general allometric  
438 functions for Norway spruce stumps and roots in Sweden (Marklund, 1988). Since Marklund's functions (1988)  
439 underestimate belowground biomass by 11 %, a factor to correct for this was included (Petersson and Ståhl,  
440 2006). Furthermore, the finest root fraction ( $\leq 2$  mm), which is not included in the functions of Marklund (1988)  
441 and Petersson and Ståhl (2006), was assumed to be 20% of needle biomass at Asa and 33% at Flakaliden,  
442 respectively, based on data from Helmisaari et al. (2007).

443

444 Data on element concentrations in biomass were available from measurements on harvested trees (S. Linder,  
445 unpublished data). At Flakaliden, total element concentrations were analysed in trees sampled for  
446 biomassdetermination in 1992 and 1997. Analyses of needles and branches (dead and live) were conducted on  
447 the same tree parts in the biomass sampled in 1993 and 1998. Base cation concentrations in biomass were  
448 determined from acid wet digestion in HNO<sub>3</sub> and HClO<sub>4</sub>, followed by determination of elements by ICP-atomic  
449 emission spectrophotometry (ICP-AES) (Jobin Yvon JY-70 Plus).

450

451 Data on element concentrations in belowground biomass fractions were taken from literature from the Nordic  
452 countries (Hellsten et al., 2013). Specifically, data on stump and root biomass of Norway spruce were available  
453 for Asa and data from Svartberget was used for Flakaliden (Table 7 in Hellsten et al., 2013).

#### 454 **2.5.5. Leaching, $L_i$**

455 Base cation leaching was quantified in six-month intervals from modelled daily runoff multiplied by average  
456 element concentrations in soil water collected with tension lysimeters at 50 cm soil depth.

457  
458 Soil water was collected from five ceramic tension lysimeters (P80) installed at 50 cm depth in each  
459 experimental plot. Soil water was collected during frost-free seasons, applying an initial tension of 70 kPa in 250  
460 mL sampling bottles, and left overnight. These soil water samples were pooled by plot. The base cation  
461 concentration in the soil solution was determined with ICP-AES. Soil water sampling was performed twice  
462 every year, i.e. in the spring and in the autumn, which are the periods of highest water flux so that the most  
463 important leaching events were covered. The spring samples were collected soon after the snowmelt and  
464 depending on the weather in a specific year this meant that the yearly spring sampling date varied between the  
465 last week of April and the last week of May. The autumn samples were collected when frost risk increased. That  
466 meant that the autumn sampling dates varied from year to year, i.e. from the first week in September to mid-  
467 November. The seasonal variation in soil water chemistry is shown in Fig. S2.

468  
469 The drainage flux out of the profile was calculated by the CoupModel (Jansson, 2012). The model was  
470 parameterised based on hydraulic soil properties measured at the sites. The model was run with hourly mean  
471 values of locally measured climate variables (precipitation, global radiation, wind speed, air temperature and  
472 humidity) and model outcomes were tested against tensiometer data, i.e. bi-weekly tensiometer readings at 15,  
473 30 and 45 cm depth were used for model calibration. The parameters were then adjusted slightly to obtain good  
474 agreement between measured and calculated soil water content. Annual precipitation varied considerably during  
475 the period 1990-2002, ranging from 906 to 504 mm at Flakaliden (mean 649 mm) and from 888 to 575 mm at  
476 Asa (mean 736 mm). Annual evapotranspiration increased by about 50 mm at both sites, during the period 1987-  
477 2003 at Flakaliden and 1990-2002 at Asa, due to the increment in tree leaf area. Monthly means and standard  
478 deviation of drainage (mm) at 50 cm depth in the soil of control plots at Asa during 1990 – 2004 and at  
479 Flakaliden during 1988–2004 are shown in Fig. S3.

#### 480 **2.5.6. Assessment of data quality in base cation budget**

481 The precision and accuracy of a base cation budget estimate of  $W_{\text{budget}, i}$  was determined by the quality of  
482 estimates of each individual term in Eq. (3), in proportion to the magnitude of each term (Simonsson et al.,  
483 2015). Significant uncertainty in the estimate of a quantitatively important term will therefore dominate the  
484 overall uncertainty in estimates of  $W_{\text{budget}}$ . Firstly, the quality of data for each term in Eq. (3) was assessed based  
485 on the spatial and temporal scales of measurements and the quality of measurements (Table 5). Using these  
486 criteria, we consider the estimates of deposition, leaching and accumulation in biomass to be of moderate to high  
487 quality. The measurements of changes in extractable soil pools were of lower quality because extraction methods  
488 were not identical for samples collected 1986/1988 and 1998/2004, which would cause significant uncertainty if  
489 soil changes were an important part of the element budget. To partly overcome this uncertainty, we used the  
490 estimates obtained by the PROFILE ( $W_{\text{profile}, i}$ ) and depletion method ( $W_{\text{depletion}, i}$ ) in additional base cation  
491 budget calculations where the change in soil was determined from the base cation budget. These additional base  
492 cation budget estimates, which are conceptually analogous to the regional mass balances presented by Akselsson  
493 et al. (2007), were also used to place the PROFILE and depletion method estimates of  $W_i$  in the context of other  
494 base cation fluxes at the ecosystem scale.

#### 495 **2.6 Statistical analyses**

496 Site mean values and standard error (SE) of  $W_{\text{depletion}}$  and  $W_{\text{profile}}$  were calculated based on the four (or two) soil  
 497 profiles studied at each site. For  $W_{\text{budget}}$  an average based on the four control plots at each site was calculated as  
 498 well as a combined standard uncertainty. The latter was partly based on standard errors derived from plot-wise  
 499 replicated data of the present experiments (for leaching and changes in exchangeable soil pools,  $SE(L_i)$  and  
 500  $SE(\Delta S_i)$ , respectively), partly on standard uncertainties ( $u$ ) derived from Simonsson et al. (2015), where  
 501 replicated data were missing in the present study (for accumulation in biomass and total deposition,  $u(\Delta B_i)$  and  
 502  $u(TD_i)$ , respectively). Because total deposition and bioaccumulation differed substantially from those in the  
 503 study of Simonsson et al. (2015), relative standard uncertainties were derived from that study, and multiplied  
 504 with the average deposition and bioaccumulation rates at Asa and Flakaliden, respectively, to yield realistic  
 505 standard uncertainties for the present sites. For the weathering rate of the  $i$ th base cation according to Eq. (4), a  
 506 combined standard uncertainty ( $u_c$ ) was calculated as:

$$507 \quad u_c(W_{\text{budget}, i}) = \sqrt{(SE(L_i))^2 + (u(\Delta B_i))^2 + (SE(\Delta S_i))^2 + (u(TD_i))^2} \quad \text{Eq. 4}$$

508 Confidence intervals were calculated by multiplying the combined standard uncertainties with a coverage factor  
 509 of 3.

### 510 3. Results

#### 511 3.1 Depletion method estimates of historical weathering rates

512 At both Asa and Flakaliden, historical weathering rates estimated with the depletion method ( $W_{\text{depletion}}$ ) were  
 513 highest in the upper soil horizons and showed a gradual decrease down to the reference depth, which was  
 514 defined at 60-70 cm at Flakaliden and for most plots at 80-90 cm at Asa (Fig. 3). Flakaliden had a higher  
 515 historical annual weathering rate to 90 cm soil depth,  $37.8 \text{ mmol}_c \text{ m}^{-2} \text{ yr}^{-1}$ , than Asa,  $12.8 \text{ mmol}_c \text{ m}^{-2} \text{ yr}^{-1}$ ; the  
 516 corresponding value for 0-50 cm depth was  $34.1 \text{ mmol}_c \text{ m}^{-2} \text{ yr}^{-1}$  at Flakaliden and  $10.5 \text{ mmol}_c \text{ m}^{-2} \text{ yr}^{-1}$  at Asa. The  
 517 gradients with depth showed that  $W_{\text{depletion}}$  increased towards the surface, although this trend was more  
 518 pronounced at Flakaliden than at Asa. At Flakaliden,  $W_{\text{depletion}}$  was highest for Mg, followed by Ca, Na and K  
 519 (Figs. 3 and 4); at Asa, it was highest for Ca, closely followed by Mg, Na and K (Figs. 3 and 4).

#### 520 3.2 PROFILE model estimates of steady state weathering rates

521 The steady state weathering rate estimated by the PROFILE model ( $W_{\text{profile}}$ ) differed from the historical rate with  
 522 respect to all three test criteria, i.e. (1) total weathering rate in the 0-50 cm soil horizon, (2) variation in  
 523 weathering with depth and (3) ranking order of base cations (Figs. 3 and 4). Firstly, regarding base cation  
 524 weathering rate in the upper 50 cm of the mineral soil,  $W_{\text{profile}}$  estimates for Asa and Flakaliden (Asa:  $37.1 \text{ mmol}_c$   
 525  $\text{m}^{-2} \text{ yr}^{-1}$ , Flakaliden:  $42.7 \text{ mmol}_c \text{ m}^{-2} \text{ yr}^{-1}$ ) were around 3.5 and 1.3-fold higher than  $W_{\text{depletion}}$  estimates,  
 526 respectively. Secondly, the total modelled base cation weathering rate for the soil profile down to 90 cm was  
 527 around 7-fold higher than the rate estimated using the depletion method at Asa ( $89.4 \text{ mmol}_c \text{ m}^{-2} \text{ yr}^{-1}$ ), and 3.4-  
 528 fold higher at Flakaliden ( $127.6 \text{ mmol}_c \text{ m}^{-2} \text{ yr}^{-1}$ ). Unlike the historical weathering based on the depletion method,  
 529 PROFILE predicted that weathering rates increased with soil depth at both sites. At Flakaliden, high contents of  
 530 K- and Mg-bearing tri-octahedral mica (Casetou-Gustafson et al., 2018) gave rise to particularly high weathering

531 rates at 70-80 cm. Thirdly, in contrast to  $W_{\text{depletion}}$ ,  $W_{\text{profile}}$  was largest for Na at both sites, followed by Ca.  
532 However,  $W_{\text{profile}}$  was larger for K than for Mg at Asa, while the reverse was true at Flakaliden.

533  
534 The sensitivity analysis of the PROFILE model using homogeneous soil physical and/or mineralogical properties  
535 demonstrated that the variations in soil physical properties (i.e. soil bulk density and specific exposed mineral  
536 surface area) with depth had a greater influence than mineralogy on the observed change in  $W_{\text{profile}}$  with soil  
537 depth. In terms of the ratios of sums of squares, the 'homogenous soil physics' scenario (1) produced 75% or  
538 more of the error obtained with 'homogenous soil physics and mineralogy' (scenario (3)), leaving a mere 25% or  
539 less to the 'homogenous mineralogy' of scenario (2); also see Figures S4 and S5. The soil physical inputs that  
540 were most important for PROFILE weathering rates are indicated in Figs. S4 and S5. There was a strong linear  
541 and positive relationship between exposed mineral surface area and  $W_{\text{profile}}$  for all elements at both sites, with  $R^2$   
542 values ranging from 0.65 to 0.89 (Fig. S6). The relationship between bulk density and  $W_{\text{profile}}$  was also strong  
543 and showed the same linear response, although  $R^2$  values were lower, 0.40-0.70 (Fig. S7).

### 544 3.3 Base cation budget estimates of current weathering rates

545 A comparison of weathering rates estimated by base cation budgets ( $W_{\text{budget}}$ ),  $W_{\text{profile}}$  and  $W_{\text{depletion}}$  was made for  
546 the 0–50 cm soil horizon. For most elements,  $W_{\text{budget}}$  in the 0–50 cm horizon was higher, or much higher, than  
547  $W_{\text{profile}}$  (Fig. 5). Compared with the PROFILE model estimates, the base cation budget estimates of weathering  
548 were 6- to 7-fold higher for Ca, Mg and K weathering at Asa, and about 2- to 3-fold higher for Ca, Mg and K at  
549 Flakaliden. At Asa, the sum of base cations was on average 13-fold and 3.6-fold larger than  $W_{\text{depletion}}$  and  $W_{\text{profile}}$ ,  
550 respectively. The closest resemblance between methods was found between  $W_{\text{depletion}}$  and  $W_{\text{budget}}$  for Na. The  
551 budget calculations suggested that weathering was a dominant source of K and Mg, but contributed a somewhat  
552 smaller proportion of Ca (61% at Asa and 43% at Flakaliden).

553  
554 As to the fluxes (terms) of the base cation budget, Na showed patterns different from those of K, Mg and Ca  
555 (Fig. 6). For Na, uptake in biomass was negligible and leaching was the dominant sink. For the K, Mg and Ca,  
556 accumulation in biomass was the dominant sink. Loss by leaching was negligible for K, but significant for Mg  
557 and Na. Deposition generally represented only a small input, except for Na at Asa. The measured decreases in  
558 soil stocks of exchangeable base cations indicated that a change in this pool was a particularly important source  
559 of Ca. There were minor increases in exchangeable stocks for Na, K and Mg at Asa. Compared to Na and Mg,  
560 the combined uncertainty of  $W_{\text{budget}}$  was larger for Ca and K, both dominated by the bioaccumulation term in Eq.  
561 (4), than for Na and Mg (Table 6). In relation to the mean  $W_{\text{budget}}$ , the combined uncertainty was of the same  
562 order of magnitude for Na, about the half for Ca, one-third for K, and lower for Mg.

563  
564 By using the weathering estimates obtained with PROFILE and the depletion method in the base cation budget  
565 equation, Eq. (4), in combination with measured estimates of deposition, leaching and uptake in biomass,  
566 alternative soil balances were estimated (Fig. 6). Since the base cation budget method predicted much higher  
567 weathering rates than the other methods, a balance of sources and sinks consequently required more marked  
568 decreases in exchangeable soil stocks for K, Ca and Mg when weathering rates were based on PROFILE or the



569 depletion method. Furthermore, as a consequence of the substantially higher  $W_{\text{profile}}$  for Na, the PROFILE based  
570 base cation budget suggested substantial increases in exchangeable Na stocks.

#### 571 **4. Discussion**

572 In spite of the fact that this study was well harmonised at the spatial scale and originated from sites with similar  
573 soil parent material, our comparison of three approaches to estimate weathering rates showed significant  
574 discrepancies between them. Discrepancies were demonstrated for all three test criteria: the sum of weathering  
575 rates in the 0–50 cm horizon, the depth gradient of weathering within this horizon, and the element rank-order of  
576 weathering rates. In the following, the discrepancies between the depletion method and the PROFILE method is  
577 first analysed because all three test criteria can be applied.

#### 578 **4.1 First test: Lower weathering rates by the depletion method compared to PROFILE**

579 Modelled ( $W_{\text{profile}}$ ) and historical ( $W_{\text{depletion}}$ ) base cation weathering rates were within the range of recently  
580 published data for similar forest sites on podzolised glacial till (Stendahl et al., 2013). However, the historical  
581 weathering rates at Asa were similar to the lowest historical weathering rate observed by Stendahl et al. (2013)  
582 and the historical weathering rates for Flakaliden were similar to their highest rates, at least with regard to Ca  
583 and Mg. The overall  $W_{\text{profile}}$  in the 0–50 cm depth was higher than  $W_{\text{depletion}}$  for Na and K. Similarly, high ratios  
584 of  $W_{\text{profile}}/W_{\text{depletion}}$  were found at catchment scale by Augustin et al. (2016). At the pedon scale, Stendahl et al.  
585 (2013) found  $W_{\text{profile}}/W_{\text{depletion}}$  ratios of on average 2.7 for 16 Swedish study sites (with average max. and min.  
586 ratios of 7.9 and 0.4, respectively); this ratio was larger than the one found for Flakaliden in our study (1.5) and  
587 lower than the one found for Asa (5.1). Similar to Flakaliden, low ratios have been reported for the Lake  
588 Gårdsjön site situated in south-western Sweden (Sverdrup et al., 1998; Stendahl et al., 2013). An exception to  
589 the general trend of higher steady-state PROFILE weathering rates compared to historical rates calculated by the  
590 depletion method, was found for Mg at the Flakaliden site, where  $W_{\text{depletion}}$  was 1.9-fold greater than  $W_{\text{profile}}$  in  
591 the upper mineral soil, but only at Flakaliden. This exception with regard to Mg was also found by Stendahl et  
592 al. (2013) for all of their 16 study sites.

593  
594 The observed discrepancy between  $W_{\text{profile}}$  and  $W_{\text{depletion}}$  has both conceptual and random origin, where the  
595 conceptual origin is due to the different temporal scales. In contrast to the observed discrepancies referred to  
596 above, several studies have concluded that the average historical weathering rate should generally be higher than  
597 the present weathering rate, since soil development involves loss of easily weatherable minerals and ageing of  
598 mineral surfaces (Bain et al., 1993; Taylor and Blum, 1995; White et al., 1996). In a study using the Historic-  
599 SAFE model, applied to the Lake Gårdsjön catchment in southwestern Sweden, Sverdrup et al. (1998) predicted  
600 a decline in weathering rates due to assumed disappearance of fine particles and loss of minerals. Their results  
601 suggested an increase in weathering rates from deglaciation 12,000 years B.P. towards a peak at 9000 years B.P.,  
602 followed by a gradual decrease to below initial levels.

603  
604 The particularly low  $W_{\text{depletion}}$  at Asa was largely attributed to a weakly developed depth gradient of Zr in the soil  
605 (Fig. 3). This observation has probably a random rather than a conceptual origin, because it might have been the  
606 result of soil mixing by different means. Mechanical soil scarification was carried out at both Asa and Flakaliden

607 prior to planting of the present stand, which would at least have caused partial mixing or inversion of surficial  
608 soil horizons. In addition, clearance cairns of unknown age were found in the experimental area at Asa,  
609 indicating small-scale agriculture in the past. Moreover, if burrowing earthworms have been abundant in the  
610 past, they might have produced soil mixing in the upper soil horizons (Taylor et al., 2019), resulting in a  
611 disturbed Zr gradient and in low estimates of historical weathering in the rooting zone (Whitfield et al. 2011).  
612 High or near-neutral soil pH and deciduous litter can promote high population densities of burrowing  
613 earthworms following forest clearing and agriculture; and we note that partly deciduous vegetation dominated at  
614 Asa until only 1000-2000 years BP, with species such as *Corylus avellana* (L.), *Betula* spp., *Quercus* spp. and  
615 *Tilia* spp. (Greisman et al., 2009).

616  
617 Apart from disturbances, natural heterogeneity in texture or mineralogy probably influenced the estimate of  
618  $W_{\text{depletion}}$  at the study sites, i.e., biases of random nature. At Flakaliden, it was reasoned that heterogeneous Zr  
619 gradients (Fig. 3) and Zr/base cation ratios (Fig. S1) disqualified two soil profiles from further analysis, which  
620 would have otherwise indicated unreasonable net gains of elements in the rooting zone (0–50 cm) (i.e. for soil  
621 profile 15A for all elements and for soil profile 11B with regard to Na and K). Whitfield et al. (2011) used the  
622 same argument for excluding single profiles from their calculations, emphasizing that overall gains in the rooting  
623 zone are not expected without external additions of base cations to the soil profiles. Several alternative reasons  
624 could have contributed to the observed peaks of Zr in the B/C-horizon at Flakaliden, such as local  
625 heterogeneities of the deposited till, which was suggested by the unstable Ti/Zr ratio in soil profile 15A and 11B.  
626 However, the observed peaks in the Ti/Zr gradients were only explained by irregularities in Ti gradients (i.e.  
627 increases in the Ti/Zr ratio indicate that Ti concentrations are increasing) the latter has to be treated carefully  
628 since in cases where both Zr and Ti show inconsistent patterns with soil depth, the Ti/Zr ratio will still be  
629 uniform and hereby overshadows heterogeneities observed with soil depth for both elements (Fig. 2, 3). Thus,  
630 heterogeneities in Zr gradients observed in the B/C horizon can be attributed to local heterogeneities of the  
631 parent material irrespective of if the Ti/Zr gradients are uniform at these depths.

632  
633 Regardless of errors in the Zr gradients, both  $W_{\text{depletion}}$  and  $W_{\text{profile}}$  showed more marked gradients with soil depth  
634 at Flakaliden compared to Asa. This could be expected based on the more well-developed podzol profile at  
635 Flakaliden. It has been postulated that the formation of podzols is enhanced by long duration and great depth of  
636 snow cover (Jauhiainen, 1973; Schaetzl and Isard, 1996), which would imply that soil formation had progressed  
637 further at Flakaliden than at Asa (Lundström et al., 2000). At Flakaliden, the average mass loss of Ca and Mg  
638 was 4.0-fold larger in the E-horizon than in the B-horizon, which is similar to findings by Olsson and Melkerud  
639 (2000) of a 5-fold higher ratio between losses of base cations in the E- compared with the B-horizon.

#### 640 **4.2 Second test: PROFILE and depletion method produce different weathering gradients in the soil**

641 Our second test, postulating similarity between  $W_{\text{depletion}}$  and  $W_{\text{profile}}$  concerning the weathering rate gradient with  
642 soil depth, was not fulfilled. This discrepancy was basically of conceptual nature. We may imagine a front of  
643 intense weathering moving downward through the soil profile over the millennia. Each horizon would undergo  
644 an episode, limited in time, of intense weathering followed by slower weathering in the ageing material. The  
645 sensitivity test performed with PROFILE revealed that the model output was only little affected by the

646 differences in mineralogy between horizons. Therefore, if processes are correctly modelled with PROFILE, the  
647 notion of a weathering front should primarily be associated with changes in bulk density and exposed mineral  
648 surface area, as also suggested by the positive correlation between  $W_{\text{profile}}$  and exposed mineral surface area and  
649 bulk density (Figs. S6-S7) and by the findings of Jönsson et al. (1995).

650

651 The increase in weathering rate with soil depth simulated by PROFILE is obviously in contrast with the classic  
652 notion of weathering rates being highest in the A- or E-horizon of podzolised soils (Tamm, 1931). To test  
653 whether the high  $W_{\text{profile}}$  values could be reconciled with the observed historical weathering, the hypothetical  
654 time needed for the PROFILE weathering rates to accomplish the element losses determined with the depletion  
655 method was calculated. This showed that the the highest weathering rate, presently prevailing at approximately  
656 80 cm (Asa) or 60 cm (Flakaliden) depth according to PROFILE (Fig. 4), would cause the observed depletion  
657 losses within less than half of the soil age ('max rates' in Fig. 7), potentially in concert with the concept of a  
658 weathering front. However, the calculation also showed that the present minimum weathering rate, presently  
659 simulated for the topmost 1-3 horizons (Fig. 4), would often result in a more severe base cation depletion within  
660 less than the postglacial period than observed by the depletion method ('min rates' in Fig. 7), particularly at  
661 Flakaliden, and for K and Na also at Asa. Hence, even considering the concept of a possible weathering front,  
662 there appears to be a positive bias in  $W_{\text{profile}}$  at the investigated sites.

#### 663 **4.3 Third test: Depletion method and PROFILE resulted in different element rank-order**

664 The weathering rates of PROFILE may also be criticized based on discrepancies in the ranking order of the  
665 weathering of elements, compared to historical weathering; this is our third test criterion. At both sites,  
666 PROFILE predicted the highest steady-state weathering for Na at both sites. However, historical weathering at  
667 Asa was greatest for Ca among the base cation elements, whilst Mg was the most abundant element released at  
668 Flakaliden. The latter was also found by Olsson and Melkerud (2000), who reported the same ranking order of  
669 individual base cation weathering (i.e.  $\text{Mg} > \text{Ca} > \text{Na} > \text{K}$ ) for other sites in northern Sweden. At the mineralogical  
670 level, Casetou-Gustafson et al. (2019) demonstrates that K-feldspar was the dominant source of all steady state  
671 PROFILE weathering of K and previous results from similar soils suggest that the dissolution rate for K-feldspar  
672 is too high compared with mica. For example, Thompson and Ukrainczyk (2002) described differences in the  
673 plant availability of K via weathering from these two mineral groups. In addition, Simonsson et al. (2016) found  
674 that, although K-feldspar contained approximately 90% of the bulk K in the soil, 25–50% of the weathering of K  
675 had occurred in mica. Furthermore, and in more general terms, Hodson and Langan (1999) suggested that the  
676 PROFILE model overestimates weathering rates because it does not consider the decrease in mineral reactivity  
677 that has taken place over time and because it assumes that all mineral surface areas are reactive. Therefore,  
678 PROFILE can be expected to overestimate base cation weathering rates, an error that can be attributed to a  
679 combination of conceptual (conditions or processes inaccurately represented in model) and random (lack of  
680 relevant field data) sources.

681

#### 682 **4.4 Weathering in a base cation budget perspective**

683 The base cation budget approach consistently resulted in much higher weathering rates than PROFILE and the  
684 depletion method for all base cations except Na. However, as was shown by the large combined uncertainties  
685 given in Table 6, base cation budget estimates of weathering are associated with substantial uncertainties from  
686 different sources. In general, significant uncertainties in the element budget of ecosystems are common (Yanai et  
687 al., 2010), and similarly large uncertainties associated with estimates of  $W_{\text{budget}}$  were observed by Simonsson et  
688 al. (2015) for the Skogaby site in south-western Sweden, a Norway spruce site of similar stand age and soil  
689 condition as Asa. Accounting for all sources of uncertainty, they found that the 95% confidence interval in  
690 estimates of base cation weathering was 2.6 times the mean ( $33 \text{ mmol}_c \text{ m}^{-2} \text{ yr}^{-1}$ ).

691  
692 Despite the considerable uncertainties in  $W_{\text{budget}}$  estimates, the base cation budget approach showed that  
693 accumulation in biomass was a dominant sink for all base cation elements except Na, in line with findings of  
694 Nykvist (2000) for two Norway spruce sites in Sweden and the findings of Simonsson et al. (2015). However,  
695 this contrasts to other studies, which assumed no change in soil and tree biomass stocks of base cations over time  
696 (e.g. Sverdrup et al., 1998). The higher estimated weathering rate at Asa reflected the higher productivity and  
697 nutrient demand of the stand at this site (Bergh et al., 1999), which has resulted in 1.4-fold greater accumulation  
698 of base cations in biomass than at Flakaliden.

699  
700 Calcium and Mg uptake in forest trees is considered to be more or less passive flow driven by transpiration  
701 fluxes, whereas K uptake is an energy-demanding active process (Nieves-Cordones et al., 2014). Considering  
702 that Na was the dominant base cation in the soil solution at 50 cm soil depth (Fig. 6), the negligible  
703 accumulation of Na in tree biomass suggests that Na uptake in trees is physiologically blocked. Low  
704 concentrations of Na seem to be a general feature of terrestrial plants in boreal forests, in contrast to aquatic  
705 plants, which explains why the latter are considered important Na sources for large herbivores like moose  
706 (Ohlson and Staaland, 2001). Thus, as in agreement with findings by e.g. Taylor and Velbel (1991) and Velbel  
707 (1995) for other types of forest ecosystems, the negligible Na accumulation in tree biomass and the particularly  
708 low deposition at Flakaliden simplify the Na budget to include only three major counterbalancing fluxes:  
709 weathering, deposition and leaching. Because  $W_{\text{depletion}}$  and  $W_{\text{budget}}$  of Na were fairly similar, and were much  
710 lower than  $W_{\text{profile}}$ , our results provide additional support for the claim that the PROFILE model produced  
711 consistently too high Na weathering.

712  
713 Accumulation in biomass was the dominant sink for Ca, Mg and K, and this term in the BC budget was  
714 considered to be of moderate to high quality (Table 5). The changes observed in extractable Ca stocks in the soil  
715 was considered more uncertain (Table 5), but they are consistent with observations over 22 years of aggrading  
716 Norway spruce forests by Zetterberg et al. (2016), who reported exchangeable Ca depletion rates of 5-11 and 23-  
717 39  $\text{mmol}_c \text{ m}^{-2} \text{ yr}^{-1}$  for sites in south-western and northern Sweden, respectively. The higher value for the northern  
718 site reflected higher Ca saturation in the soil. The corresponding values for Asa and Flakaliden were larger, but  
719 of similar magnitude (34.5 and 40.5  $\text{mmol}_c \text{ m}^{-2} \text{ yr}^{-1}$ , respectively). Brandtberg and Olsson (2012) studied the  
720 same sites as Zetterberg et al. (2016) over a 10-year period and found a general minor increase in exchangeable  
721 K soil stocks and a substantial decrease in the Ca stocks, a result much similar to the findings of the present  
722 study.

723

724 When an independent estimate of current weathering rate ( $W_{\text{profile}}$ ) is introduced in the budget (Fig. 6) the high  
725 rate of accumulation in biomass is not explained by the combination of measured ( $TD, \Delta S$ ) or modelled ( $W_{\text{profile}}$ )  
726 sources or sinks ( $L$ ). This result suggests that forest trees have access to additional sources of Ca, Mg and K, not  
727 measured or captured by our study. We can only speculate about the nature of such sources: It is possible that  
728 depletion of ammonium-chloride-exchangeable base cations underestimates the plant-available phases of BC in  
729 the soil. Using other extract media than  $\text{NH}_4\text{Cl}$  may have revealed additional sources from e.g. oxalates  
730 (Rosenstock et al., 2019b). Additional BC release from decomposing roots, stumps and residues from the felling  
731 of the former stand was probably neglected because of difficulties to include coarse wood in soil sampling. It is  
732 also possible that the assumption made that no base cation uptake takes place below 50 cm in the soil was  
733 wrong. If trees can take up base cations from deeper soil horizons (e.g. Callesen et al., 2016; Brantley et al.,  
734 2017), the discrepancy in weathering rates between the two methods would be reduced since PROFILE predicted  
735 higher weathering rates with increasing depth. Furthermore, although biological processes are represented in  
736 PROFILE, the model fail to capture biological feedback mechanisms in their entirety, in particular feedbacks  
737 generated by plant uptake and mycorrhiza (Finlay et al., 2009; Sverdrup, 2009; Smits and Wallander, 2017;  
738 Akselsson et al., 2019; Finlay et al., this issue; Rosenstock et al. 2019a).

## 739 5. Conclusions

740 A general observation from our comparison of three conceptually different methods was that weathering rate  
741 estimates were lower by the depletion method than the PROFILE model for the 0–50 cm soil horizon, and that  
742 the highest weathering rates were estimated by the BC budget approach. In sharp contrast to the historic  
743 weathering estimated by the depletion method, the current steady-state weathering by PROFILE increased with  
744 increasing soil depth.

745

746 The Na weathering rate was an important exception from the general finding as PROFILE estimated much  
747 higher weathering rate for Na than the other methods, which produced similar weathering rates for Na. This  
748 indicated that the high weathering rate of Ca, Mg and K by the budget method was at large an effect of high  
749 nutrient demand and uptake rate of these elements in the aggrading forest stands. Hence, weathering rates of Ca,  
750 Mg and K by the budget method were in our case most likely overestimated. An implication of this conclusion is  
751 that forest trees probably have access to additional sources of nutrients base cation, not measured or captured by  
752 our study.

753

754 Another implication of the higher weathering rate for Na by PROFILE compared to the other methods is that the  
755 model may have overestimated release rates of Na, and probably also of K. This conclusion was based on  
756 differences between historical and steady-state estimates regarding the rank-order of elements, and the fact that  
757 even the lowest PROFILE weathering rates were too high compared with observed depletions of Na and K. A  
758 possible cause to the fact that K weathering rates were overestimated by the PROFILE method was incorrect  
759 parameters for the weathering of K-bearing minerals in the model, which should be accounted for in future  
760 PROFILE based weathering estimate.

761

762 The depletion method resulted in generally lower weathering rates at Asa than at Flakaliden, whereas the  
763 PROFILE estimates for the sites were more similar, indicating that historical weathering estimated by the  
764 depletion method was probably underestimated at Asa. This was an effect of the weakly developed and possibly  
765 erratic Zr gradients in the soil at Asa, which could have been caused by natural and anthropogenic disturbances.  
766 Future studies based on the depletion method should ensure that the Zr gradient with depth show a net  
767 enrichment of Zr towards the soil surface. This condition was not fulfilled for soil profiles at the Asa site.  
768 Another important outcome of the study was to show that within-site variations in Zr gradients can be large, as  
769 was the case at Flakaliden for two soil profiles.

## 770 **6. Authors contribution**

771 Authors contributed to the study as in the following: S. Casetou-Gustafson: study design, data treatment,  
772 analyses, interpretation and writing. Magnus Simonsson: study design, analysis, interpretation and writing. Johan  
773 Stendahl: study design, analysis, interpretation and writing B.A. Olsson: study design, data treatment, analysis,  
774 interpretation and writing. S. Hillier: interpretation and writing. Sune Linder: Provided long-term experimental  
775 data, interpretation and writing. Harald Grip: Provided long-term experimental data, interpretation, and writing.

## 776 **7. Acknowledgements**

777 Financial support from The Swedish research Council for Environment, Agricultural Sciences and Spatial  
778 Planning (212-2011-1691) (FORMAS) (Strong Research Environment, QWARTS) and the Swedish Energy  
779 Agency (p36151-1). Stephen Hillier acknowledges support of the Scottish Government's Rural and Environment  
780 Science and Analytical Services Division (RESAS). We thank Cecilia Akselsson for her contribution to study  
781 design, PROFILE model development and valuable comments on earlier versions of the manuscript.

## 782 **8. References**

- 783 Achat, D.L., Deleuze, C., Landmann, G., Pousse, N., Ranger, J., and Augusto, L.: Quantifying consequences of  
784 removing harvesting residues on forest soils and tree growth – A meta-analysis, *For. Ecol. Manage.*, 348, 124–  
785 141, 2015.
- 786 Akselsson, C., Westling, O., Sverdrup, H., Holmqvist, J., Thelin, G., Uggla, E., and Malm, G.: Impact of harvest  
787 intensity on long-term base cation budgets in Swedish forest soils, *Water Air Soil Poll.: Focus*, 7, 201-210, 2007.
- 788 Akselsson, C., Belyazid, S., Stendahl, J., Finlay, R., Olsson, B.A., Erlandsson Lampa, M., Wallander, H.,  
789 Gustafsson, J.P., and Bishop, K. H.: Weathering rates in Swedish forest soils, *Biogeosciences* 16 (in press).
- 790 Albaugh, T. J., Bergh, J., Lundmark, T., Nilsson, U., Stape, J. L., Allen, H. L., and Linder, S.: Do biological  
791 expansion factors adequately estimate stand-scale aboveground component biomass for Norway spruce? *For.*  
792 *Ecol. Manage.*, 258, 2628-2637, 2009.
- 793 Albaugh, T. J., Bergh, J., Lundmark, T., Nilsson, U., Stape, J. L., Allen, H. L., and Linder, S.: Corrigendum to  
794 “Do biological expansion factors adequately estimate stand-scale aboveground component biomass for Norway  
795 spruce?”, *For. Ecol. Manage.*, 270, 314, 2012.
- 796 Augustin, F., Houle, D., Gagnon, C., and Courchesne, F.: Evaluation of three methods for estimating the  
797 weathering rates of base cations in forested catchments, *Catena*, 144, 1-10, 2016.

798 Bailey, S. W., Buso, D. C., and Likens, G. E.: Implications of sodium mass balance for interpreting the calcium  
799 cycle of a forested ecosystem, *Ecology*, 84, 471-484, 2003.

800 Bain, D. C., Mellor, A., Robertson-Rintoul, M., and Buckland, S.: Variations in weathering processes and rates  
801 with time in a chronosequence of soils from Glen Feshie, Scotland, *Geoderma*, 57, 275-293, 1993.

802 Bain, D. C., Mellor, A., Wilson, M., and Duthie, D.: Chemical and mineralogical weathering rates and processes  
803 in an upland granitic till catchment in Scotland, *Water Air Soil Poll.*, 73, 11-27, 1994.

804 Bergh, J., Linder, S., Lundmark, T., and Elfving, B.: The effect of water and nutrient availability on the  
805 productivity of Norway spruce in northern and southern Sweden, *For. Ecol. Manage.*, 119, 51-62, 1999.

806 Bergh, J., Linder, S., and Bergström, J.: Potential production of Norway spruce in Sweden, *For. Ecol. Manage.*,  
807 204, 1-10, 2005.

808 Binkley, D., and Högberg, P.: Tamm review: revisiting the influence of nitrogen deposition on Swedish forests,  
809 *For. Ecol. Manage.*, 368, 222-239, 2016.

810 Boyle, J.R., Phillips, J.J., and Ek, A.R.: "Whole tree "harvesting: Nutrient budget evaluation. *J. Forestry*, 71,  
811 760-762, 1973.

812 Brandtberg, P.-O., and Olsson, B.A.: Changes in the effects of whole-tree harvesting on soil chemistry during 10  
813 years of stand development. *For. Ecol. Manage.*, 277, 150–162, 2012.

814 Brantley, S.L., Eissenstat, D.M., Marshall, J.A., Godsey, S.E., Balogh-Brunstad, Z., Karwan, D.L., Papuga, S.A.,  
815 Roering, J., Dawson, T.E., and Evaristo, J.: Reviews and syntheses: on the roles trees play in building and  
816 plumbing the critical zone, *Biogeosciences*, 14, 5115–5142, 2017

817 Brimhall, G. H., Ford, C., Bratt, J., Taylor, G., and Warin, O.: Quantitative geochemical approach to  
818 pedogenesis: importance of parent material reduction, volumetric expansion, and eolian influx in lateritization,  
819 *Geoderma*, 51, 51-91, 1991.

820 Callesen, I., Harrison, R., Stupak, I., Hatten, J., Raulund-Rasmussen, K., Boyle, J., Clarke, N., and Zabrowski,  
821 D.: Carbon storage and nutrient mobilization from soil minerals by deep roots and rhizospheres, *For. Ecol.*  
822 *Manage.*, 359, 322–331, 2016.

823 Casetou-Gustafson, S., Hillier, S., Akselsson, C., Simonsson, M., Stendahl, J., and Olsson, B. A.: Comparison of  
824 measured (XRPD) and modeled (A2M) soil mineralogies: A study of some Swedish forest soils in the context of  
825 weathering rate predictions, *Geoderma*, 310, 77-88, 2018.

826 Casetou-Gustafson, S., Akselsson, C., Hillier, S., and Olsson, B. A.: The importance of mineral composition  
827 determinations to PROFILE base cation release rates: A case study, *Biogeosciences* 16, 1903–1920, 2019.

828 Chadwick, O. A., Brimhall, G. H., and Hendricks, D. M.: From a black to a gray box—a mass balance  
829 interpretation of pedogenesis, *Geomorphology*, 3, 369-390, 1990.

830 De Jong, J., Akselsson, C., Egnell, G., Löfgren, S., and Olsson, B.A.: Realizing the energy potential of forest  
831 biomass in Sweden – how much is environmentally sustainable?, *For. Ecol. Manage.*, 383, 3–16, 2017.

832 Erlandsson Lampa, M., Sverdrup, H.U., Bishop, K.H., Belyazid, S., Ameli, A., and Köhler, S. J.: Catchment  
833 export of base cations: Improved mineral dissolution kinetics influence the role of water transit time,  
834 *Biogeosciences* (in review).

835 Finlay, R., Wallander, H., Smits, M., Holmström, S., Van Hees, P., Lian, B., and Rosling, A.: The role of fungi  
836 in biogenic weathering in boreal forest soils, *Fungal Biol. Rev.*, 23, 101-106, 2009.

837 Finlay, R.D., Mahmood, S., Rosenstock, N., Bolou-bi, E., Köhler, S.J., Fahad, Y., Rosling, Wallander, H.,  
838 Belyazid, S., Bishop, K., and Lian, B.: Biological weathering and its consequence at different spatial levels – from  
839 nanoscale to global scale, *Biogeosciences* (in review).

840 Fredén, C.: *The National Atlas of Sweden, Geology, Third Ed.* SNA Publishing House, Stockholm, Sweden,  
841 2009.

842 Fröberg, M., Berggren, D., Bergkvist, B., Bryant, C., and Mulder, J.: Concentration and Fluxes of Dissolved  
843 Organic Carbon (DOC) in Three Norway Spruce Stands along a Climatic Gradient in Sweden,  
844 *Biogeochemistry*, 77, 1-23, 2006.

845 Fröberg, M., Grip, H., Tipping, E., Svensson, M., Strömberg, M., and Kleja, D. B.: Long-term effects of  
846 experimental fertilization and soil warming on dissolved organic matter leaching from a spruce forest in  
847 Northern Sweden, *Geoderma*, 200, 172-179, 2013.

848 Futter, M., Klaminder, J., Lucas, R., Laudon, H., and Köhler, S.: Uncertainty in silicate mineral weathering rate  
849 estimates: source partitioning and policy implications, *Environ Res. Lett.*, 7, 024025, 2012.

850 Garrels, R.M. and Mackenzie, F.T.: Origin of the chemical compositions of some springs and lakes. In: Stumm,  
851 W. (ed.), *Equilibrium Concepts in Natural Water Systems, Advances in Chemistry Series, 67.* Am. Chem. Soc.,  
852 pp. 222–242 (Chapter 10), 1967.

853 Greisman, A., and Gaillard, M. J.: The role of climate variability and fire in early and mid Holocene forest  
854 dynamics of southern Sweden, *J. Quaternary Sci.*, 24, 593-611, 2009.

855 Grennfelt, P., and Hov, Ø.: Regional air pollution at a turning point, *Ambio*, 2-10, 2005.

856 Harden, J. W.: Soils developed in granitic alluvium near Merced, California, *Geological Survey Bulletin (USA)*  
857 1590-A, *Soil Chronosequences in the Western United States*, Government Printing Office, Washington DC,  
858 USA, A1–A65, 1987.

859 Hedin, L. O., Granat, L., Likens, G. E., Buishand, T. A., Galloway, J. N., Butler, T. J., and Rodhe, H.: Steep  
860 declines in atmospheric base cations in regions of Europe and North America, *Nature*, 367, 351-354, 1994.

861 Hedwall, P. O., Grip, H., Linder, S., Lövdahl, L., Nilsson, U., and Bergh, J.: Effects of clear-cutting and slash  
862 removal on soil water chemistry and forest-floor vegetation in a nutrient optimised Norway spruce stand, *Silva*  
863 *Fenn.*, 47, article id 933, 2013.

864 Hellsten, S., Helmisaari, H. S., Melin, Y., Skovsgaard, J. P., Kaakinen, S., Kukkola, M., Saarsalmi, A.,  
865 Petersson, H., and Akselsson, C.: Nutrient concentrations in stumps and coarse roots of Norway spruce, Scots  
866 pine and silver birch in Sweden, Finland and Denmark, *For. Ecol. Manage.*, 290, 40-48, 2013.

867 Helmisaari, H.-S., Derome, J., Nöjd, P., and Kukkola, M.: Fine root biomass in relation to site and stand  
868 characteristics in Norway spruce and Scots pine stands, *Tree Physiol.*, 27, 1493-1504, 2007.

869 Hillier, S.: Use of an air brush to spray dry samples for X-ray powder diffraction, *Clay Miner.*, 34, 127-127,  
870 1999.

871 Hillier, S.: Quantitative analysis of clay and other minerals in sandstones by X-ray powder diffraction (XRPD),  
872 In: *Clay Mineral Cements in Sandstones*, edited by: Worden, R., Morad, S.: International Association of  
873 Sedimentologists, Special Publication, John Wiley and Sons Ltd, Oxford, United Kingdom, 34, 213-251, 2003.

874 Hodson, M. E., Langan, S. J., and Wilson, M. J.: A sensitivity analysis of the PROFILE model in relation to the  
875 calculation of soil weathering rates, *Appl. Geochem.*, 11, 835-844, 1996.

876 Hodson, M. E., and Langan, S. J.: The influence of soil age on calculated mineral weathering rates, *Appl.*



877 Geochem., 14, 387-394, 1999.

878 Iwald, J., Löfgren, S., Stendahl, J., and Karlton, E.: Acidifying effect of removal of tree stumps and logging  
879 residues as compared to atmospheric deposition, *For. Ecol. Manage.*, 290, 49–58, 2013.

880 Jansson, P.-E.: CoupModel: model use, calibration, and validation, *Trans. Am. Soc. Agric. Eng.*, 55, 1337-1344,  
881 2012.

882 Jauhiainen, E.: Age and degree of podzolization of sand soils on the coastal plain of northwest Finland, *Comm.*  
883 *Biol.*, 68, 1-32, 1973.

884 Jönsson, C., Warfvinge, P., and Sverdrup, H.: Uncertainty in predicting weathering rate and environmental stress  
885 factors with the PROFILE model, *Water Air Soil Poll.*, 81, 1-23, 1995.

886 Karlsson, P. E., Ferm, M., Hultberg, H., Hellsten, S., Akselsson, C., and Pihl Karlsson, G.: Totaldeposition av  
887 kväve till skog, IVL Swedish Environmental Research Institute, Stockholm, Sweden, Report B1952,, 37 pp.,  
888 2011.

889 Karlsson, P. E., Ferm, M., Hultberg, H., Hellsten, S., Akselsson, C., and Pihl Karlsson, G.: Totaldeposition av  
890 baskatjoner till skog, IVL Swedish Environmental Research Institute, Stockholm, Sweden, Report B2058, 64  
891 pp., 2013.

892 Kellner, O.: Effects of fertilization on forest flora and vegetation, Ph.D. thesis, Comprehensive Summaries of  
893 Uppsala Dissertations from the Faculty of Science, Uppsala University, Sweden, 464, 32 pp., 1993.

894 Klaminder, J., Lucas, R., Futter, M., Bishop, K., Köhler, S., Egnell, G., and Laudon, H.: Silicate mineral  
895 weathering rate estimates: Are they precise enough to be useful when predicting the recovery of nutrient pools  
896 after harvesting?, *For. Ecol. Manage.*, 261, 1-9, 2011.

897 Kolka, R. K., Grigal, D., and Nater, E.: Forest soil mineral weathering rates: use of multiple approaches,  
898 *Geoderma*, 73, 1-21, 1996.

899 Koseva, I.S., Watmough, S.A., and Aherne, J.: Estimating base cation weathering rates in Canadian forest soils  
900 using a simple texture-based model, *Biogeochemistry*, 101, 183-196, 2010.

901 Lidskog, R. and Sundqvist, G.: The role of science in environmental regimes: The case of LRTAP, *Eur. J.*  
902 *Internat. Rel.*, 8, 77-101, 2002.

903 Likens, G. E., and Bormann, F. H.: Acid rain: a serious regional environmental problem, *Science*, 184, 1176-  
904 1179, 1974.

905 Likens, G. E., Driscoll, C. T., Buso, D. C., Siccama, T. G., Johnson, C. E., Lovett, G. M., Fahey, T. J., Reiners,  
906 W. A., Ryan, D. F., Martin, C. W., and Bailey, S. W.: The biogeochemistry of calcium at Hubbard Brook,  
907 *Biogeochemistry*, 41, 89-173, 1998.

908 Linder, S.: Foliar analysis for detecting and correcting nutrient imbalances in Norway spruce, *Ecol. Bull.*  
909 (Copenhagen), 178-190, 1995.

910 Löfgren, S., Aastrup, M., Bringmark, L., Hultberg, H., Lewin-Pihlblad, L., Lundin, L., Karlsson, G. P., and  
911 Thunholm, B.: Recovery of soil water, groundwater, and streamwater from acidification at the Swedish  
912 Integrated Monitoring catchments, *Ambio*, 40, 836-856, 2011.

913 Lundström, U., Van Breemen, N., Bain, D., Van Hees, P., Giesler, R., Gustafsson, J. P., Ilvesniemi, H., Karlton,  
914 E., Melkerud, P.-A., and Olsson, M.: Advances in understanding the podzolization process resulting from a  
915 multidisciplinary study of three coniferous forest soils in the Nordic Countries, *Geoderma*, 94, 335-353, 2000.

916 Marklund, L. G.: Biomass functions for pine, spruce and birch in Sweden, Department of Forest Survey,  
917 Swedish University of Agricultural Sciences, Umeå, Sweden, Report 45, 1–73, 1988.

918 Marshall, C. and Haseman, J.: The quantitative evaluation of soil formation and development by heavy mineral  
919 studies: A Grundy silt loam profile 1, Soil Sci. Soc. Am. J., 7, 448-453, 1943.

920 Nieves-Cordones, M., Alemán, F., Martínez, V., and Rubio, F.: K<sup>+</sup> uptake in plant roots. The systems involved,  
921 their regulation and parallels in other organisms, J. Plant Physiol., 171, 688-695, 2014.

922 Nilsson, S. I., Miller, H. G., and Miller, J. D.: Forest growth as a possible cause of soil and water acidification -  
923 an examination of the concepts, Oikos, 39, 40-49, 1982.

924 Nilsson, S.I. and Tyler, G.: Acidification-induced chemical changes of forest soils during recent decades – a  
925 review. In: Staaf, H. and Tyler, G. (eds), Effects of acid deposition and tropospheric ozone on forest ecosystems  
926 in Sweden. Ecol. Bull. (Copenhagen) 44, 54–64, 1995.

927 Nykvist, N.: Effects of clearfelling, slash removal and prescribed burning on amounts of plant nutrients in  
928 biomass and soil, Swedish University of Agricultural Sciences, Department of Forest Ecology, Uppsala,  
929 Sweden, 210, 2000.

930 Ohlson, M. and Staaland, H.: Mineral diversity in wild plants: benefits and bane for moose, Oikos, 94, 442-454,  
931 2001.

932 Olsson, B. A., Bengtsson, J., and Lundkvist, H.: Effects of different forest harvest intensities on the pools of  
933 exchangeable cations in coniferous forest soils, For. Ecol. Manage., 84, 135-147, 1996.

934 Olsson, M. and Melkerud, P.-A.: Chemical and mineralogical changes during genesis of a Podzol from till in  
935 southern Sweden, Geoderma, 45, 267-287, 1989.

936 Olsson, M. T. and Melkerud, P.-A.: Weathering in three podzolized pedons on glacial deposits in northern  
937 Sweden and central Finland, Geoderma, 94, 149-161, 2000.

938 Omotoso, O., McCarty, D. K., Hillier, S., and Kleeberg, R.: Some successful approaches to quantitative mineral  
939 analysis as revealed by the 3rd Reynolds Cup contest, Clay Clay Miner., 54, 748-760, 2006.

940 Ouimet, R. and Duchesne, L.: Base cation mineral weathering and total release rates from soils in three  
941 calibrated forest watersheds on the Canadian Boreal Shield, Can. J. Soil Sci. 85, 245–260, 2005.

942 Paré, D., Rochon, P., and Brais, S.: Assessing the geochemical balance of managed boreal forests, Ecol.  
943 Indicators 1, 293–311, 2002.

944 Petersson, H., and Ståhl, G.: Functions for below-ground biomass of *Pinus sylvestris*, *Picea abies*, *Betula*  
945 *pendula* and *Betula pubescens* in Sweden, Scand. J. For. Res., 21, 84-93, 2006.

946 Phelan, J., Belyazid, S., Kurz, D., Guthrie, S., Cajka, J., Sverdrup, H., and Waite, R.: Estimation of soil base  
947 cation weathering rates with the PROFILE model to determine critical loads of acidity for forested ecosystems in  
948 Pennsylvania, USA: Pilot application of a potential national methodology, Water Air Soil Pollut., 225:2109,  
949 2014. DOI 10.1007/s11270-014-2109-4

950 Ranius, T., Hämäläinen, A., Egnell, G., Olsson, B., Eklöf, K., Stendahl, J., Rudolphi, J., Sténs, A., and Felton,  
951 A.: The effects of logging residue extraction for energy on ecosystem services and biodiversity: A synthesis, J.  
952 Environ. Manage., 209, 409–425, 2018.

953 Reuss, J. O., and Johnson, D.W.: Acid deposition and the acidification of soils and waters, Ecol. Stud., 95, 1986.

954 Rosenstock, N.P., van Hees, P.A.W., Fransson, P.M.A., Finlay, R.D., and Rosling, A.: Biological enhancement  
955 of mineral weathering by *Pinus sylvestris* seedlings – effects of plants, ectomycorrhizal fungi, and elevated CO<sub>2</sub>,  
956 Biogeosciences, 16, 3637–3649, 2019 a.

957 Rosenstock, N.P., Stendahl, J., van der Heijden, G., Lundin, L., McGivney, E., Bishop, K., and Löfgren, S.: Base  
958 cations in the soil bank. Non-exchangeable pools may sustain centuries of net loss to forestry and leaching, Soil,  
959 (in press), 2019

960 Ryan, M. G.: Three decades of research at Flakaliden advancing whole-tree physiology, forest ecosystem and  
961 global change research, Tree Physiol., 33, 1123-1131, 2013.

962 Schaetzl, R. J. and Isard, S. A.: Regional-scale relationships between climate and strength of podzolization in the  
963 Great Lakes region, North America, Catena, 28, 47-69, 1996.

964 Schützel, H., Kutschke, D., and Wildner, G.: Zur Problematik der Genese der Grauen Gneise des sächsischen  
965 Erzgebirges (zirkonstatistische Untersuchungen), VEB Deutscher Verlag für Grundstoffindustrie, Leipzig, 1963.

966 Sigurdsson, B. D., Medhurst, J. L., Wallin, G., Eggertsson, O., and Linder, S.: Growth of mature boreal Norway  
967 spruce was not affected by elevated [CO<sub>2</sub>] and/or air temperature unless nutrient availability was improved, Tree  
968 Physiol., 33, 1192-1205, 2013.

969 Simonsson, M., and Berggren, D.: Aluminium solubility related to secondary solid phases in upper B horizons  
970 with spodic characteristics, Eur. J. Soil Sci., 49, 317-326, 1998.

971 Simonsson, M., Bergholm, J., Olsson, B. A., von Brömssen, C., and Öborn, I.: Estimating weathering rates using  
972 base cation budgets in a Norway spruce stand on podzolised soil: analysis of fluxes and uncertainties, For. Ecol.  
973 Manage., 340, 135-152, 2015.

974 Simonsson, M., Bergholm, J., Lemarchand, D. and Hillier, S.: Mineralogy and biogeochemistry of potassium in  
975 the Skogaby experimental forest, southwest Sweden: pools, fluxes and K/Rb ratios in soil and biomass,  
976 Biogeochemistry, 131, 77-102, 2016.

977 Smits, M. M. and Wallander, H.: Role of mycorrhizal symbiosis in mineral weathering and nutrient mining from  
978 soil parent material, In: Mycorrhizal Mediation of Soil: Fertility, Structure, and Carbon Storage, edited by:  
979 Johnson, N. C., Gehring, C., and Jansa, J., Elsevier, United States, 35-46, 2017.

980 Starr, M., Lindroos, A.-J., and Ukonmaanaho, L.: Weathering release rates of base cations from soils within a  
981 boreal forested catchment: variation and comparison to deposition, litterfall and leaching fluxes, Environ. Earth  
982 Sci., 72, 5101-5111, 2014.

983 Stendahl, J., Lundin, L., and Nilsson, T.: The stone and boulder content of Swedish forest soils, Catena, 77, 285-  
984 291, 2009.

985 Stendahl, J., Akselsson, C., Melkerud, P.-A., and Belyazid, S.: Pedon-scale silicate weathering: comparison of  
986 the PROFILE model and the depletion method at 16 forest sites in Sweden, Geoderma, 211, 65-74, 2013.

987 Strengbom, J., Dahlberg, A., Larsson, A., Lindelow, A., Sandström, J., Widenfalk, O., and Gustafsson, L.:  
988 Introducing intensively managed spruce plantations in Swedish forest landscapes will impair biodiversity  
989 decline, Forests, 2, 610-630, 2011.

990 Sudom, M. and St. Arnaud, R.: Use of quartz, zirconium and titanium as indices in pedological studies, Can. J.  
991 Soil Sci., 51, 385-396, 1971.

992 Sverdrup, H.: Chemical weathering of soil minerals and the role of biological processes, Fungal Biol. Rev., 23,  
993 94-100, 2009.

994 Sverdrup, H. and de Vries, W., Calculating critical loads for acidity with the simple mass-balance method, *Water*  
995 *Air Soil Pollut*, 72, 143–162, 1994.

996 Sverdrup, H., Warfvinge, P., Frogner, T., Håøya, A.O., Johansson, M., and Andersen, B.: Critical loads of  
997 acidity in the Nordic countries, *Ambio*, 21, 348–355, 1992.

998 Sverdrup, H. and Rosén, K.: Long-term base cation mass balances for Swedish forests and the concept of  
999 sustainability, *For. Ecol. Manage.*, 110, 221-236, 1998.

1000 Sverdrup, H. and Warfvinge, P.: Weathering of primary silicate minerals in the natural soil environment in  
1001 relation to a chemical weathering model, *Water Air Soil Poll.*, 38, 387-408, 1988.

1002 Sverdrup, H., Warfvinge, P., and Wickman, T.: Estimating the weathering rate at Gårdsjon using different  
1003 methods, In: *Experimental Reversal of Rain Effects: Gardsjon Roof Project*, edited by: Hultberg, H. and  
1004 Skeffington, R., John Wiley & Sons Ltd, Chichester, United Kingdom, 231-249, 1998.

1005 Tamm, O.: Studier över jordmånstyper och deras förhållande till markens hydrologi i nordsvenska  
1006 skogsterränger barrskogsområdet, *Reports of the Swedish Institute of Experimental Forestry*, 26(2), 163-355,  
1007 1931. (In Swedish)

1008 Taylor, A. and Blum, J. D.: Relation between soil age and silicate weathering rates determined from the  
1009 chemical evolution of a glacial chronosequence, *Geology*, 23, 979-982, 1995.

1010 Taylor, A., Lenoir, L., Vegerfors, B., and Persson, T.: Ant and earthworm bioturbation in cold-temperate  
1011 ecosystems, *Ecosystems*, 1-14, 2019.

1012 Taylor, A.B. and Velbel, M.A., 1991.: Geochemical mass balance and weathering rates in forested watersheds of  
1013 the southern Blue Ridge. II. Effects of botanical uptake terms. In: Pavich, M.J. (Editor), *Weathering and Soils*.  
1014 *Geoderma*, 51, 29-50.

1015 .Thiffault, E., Hannam, K.D., Paré, D., Titus, B.D., Hazlett, P.W., Maynard D.G., and Brais, S. Effects of forest  
1016 biomass harvesting on soil productivity in boreal and temperate forests – A review, *Environ. Review* 19(NA),  
1017 278-309, 2011.

1018 Thompson, M. L. and Ukrainczyk, L.: Micas, *Soil mineralogy with environmental applications*, in: *Soil*  
1019 *Mineralogy with Environmental Applications*, edited by: Dixon, J. B., and Schulze, D. G., Soil Science Society  
1020 of America Inc., Madison, 431-466 pp., 2002.

1021 Van Der Salm, C.: Assessment of the regional variation in weathering rates of loess and clay soils in the  
1022 Netherlands, *Water Air Soil Poll.*, 131, 217-243, 2001.

1023 Velbel, M. A.: Geochemical mass balances and weathering rates in forested watersheds of the southern Blue  
1024 Ridge, *Am. J. Sci.*, 285, 904-930, 1985.

1025 Velbel, M.A., 1995.: Interaction of ecosystem processes and weathering. In: Trudgill, S., (Editor),  
1026 *Solute Modelling in Catchment Systems*, John Wiley & Sons, pp. 193-209.

1027 Velbel, M.A. and Price, J.R.: Solute geochemical mass-balances and mineral weathering rates in small  
1028 watersheds: methodology, recent advances and futures directions, *Appl. Geochem.*, 22, 1682–1700, 2007.

1029 Viro, P.: Kivisyiden maarittamisesta, Summary: On the determination of stoniness, *Commun. Inst. For. Fenn.*,  
1030 40, 8, 1952.

1031 Warfvinge, P., and Sverdrup, H.: *Critical Loads of Acidity to Swedish Forest Soils: Methods, Data and Results*,  
1032 *Reports in Ecology and Environmental Engineering*, Dpt. of Chemical Engineering II, Lund University, Lund,  
1033 Sweden, 1995.

1034 White, A. F., Blum, A. E., Schulz, M. S., Bullen, T. D., Harden, J. W., and Peterson, M. L.: Chemical  
1035 weathering rates of a soil chronosequence on granitic alluvium: I. Quantification of mineralogical and surface  
1036 area changes and calculation of primary silicate reaction rates, *Geochim. Cosmochim. Acta*, 60, 2533-2550,  
1037 1996.

1038 Whitfield, C., Watmough, S., Aherne, J., and Dillon, P.: A comparison of weathering rates for acid-sensitive  
1039 catchments in Nova Scotia, Canada and their impact on critical load calculations, *Geoderma*, 136, 899-911,  
1040 2006.

1041 Whitfield, C. J., Watmough, S. A., and Aherne, J.: Evaluation of elemental depletion weathering rate estimation  
1042 methods on acid-sensitive soils of north-eastern Alberta, Canada, *Geoderma*, 166, 189-197, 2011.

1043 Whitfield, C. J. and Watmough, S. A.: A regional approach for mineral soil weathering estimation and critical  
1044 load assessment in boreal Saskatchewan, Canada. *Sci. Tot. Environ.*, 437, 165–172, 2012.

1045 Wikström, P., Edenius, L., Elfving, B., Eriksson, L. O., Lämås, T., Sonesson, J., Öhman, K., Wallerman, J.,  
1046 Waller, C., and Klintebäck, F.: The Heureka forestry decision support system: an overview, *Math. Comput. For.*  
1047 *Nat. Res. Sci.*, 3, 87, 2011.

1048 Yanai, R.D., Battles, J.J., Richardson, A.D., Blodgett, C.A., Wood, D.M., and Rastetter, E.B.: Estimating  
1049 uncertainty in ecosystem budget calculations. *Ecosystems*, 13, 239–248, 2010.

1050 Zetterberg, T., Olsson, B. A., Löfgren, S., von Brömssen, C., and Brandtberg, P. O.: The effect of harvest  
1051 intensity on long-term calcium dynamics in soil and soil solution at three coniferous sites in Sweden, *For. Ecol.*  
1052 *Manage.*, 302, 280-294, 2013.

1053 Zetterberg, T., Olsson, B. A., Löfgren, S., Hyvönen, R., and Brandtberg, P. O.: Long-term soil calcium depletion  
1054 after conventional and whole-tree harvest, *For. Ecol. Manage.*, 369, 102-115, 2016.

1055

**Table 1.** Soil profile characteristics at 50 cm depth in the mineral soil at the Asa and Flakaliden sites

Site	Plot	Clay (wt.%)	Silt (wt.%)	Sand (wt.%)	Coarse (wt.%)	Density (g cm <sup>3</sup> )	Soil age (calender years )
Asa	K1	9.49	25.04	45.30	20.18	1.10	14300
	K4	7.65	22.59	39.21	30.48	1.09	14300
	F3	4.95	25.26	40.54	29.25	0.99	14300
	F4	8.64	25.69	40.13	25.54	0.94	14300
Flakaliden	15A	1.92	9.21	68.98	19.68	1.89	10150
	14B	7.71	34.09	33.71	24.17	1.35	10150
	10B	7.75	45.17	37.23	8.90	1.36	10150
	11B	9.56	45.07	33.91	10.72	1.47	10150

1056

1057

1058  
1059  
1060  
1061

**Table 2.** A short description of characteristics of the three different approaches that are used in the study to estimate base cation release rates at the pedon scale using a harmonized set of input data. The difference between methods reflect expected differences due to different time scales, conceptual differences, assumptions about weathering kinetics and pedogenesis.

1062

Description	PROFILE	Depletion	Base cation budget
Time scale	Present-day	Long-term	Present-day
Concept	Steady-state	Historical	Dynamic
Weathering kinetics	Long-term kinetics	No assumption	No assumption
Pedogenesis	No assumption	Zr immobility, unweathered and homogeneous parent material	No assumption

1063  
1064

1065  
1066  
1067  
1068

**Table 3.** Extractable concentrations of different elements at the reference depths used for calculating historical weathering rate at the Asa and Flakaliden sites.

Site	Plot	Ref. depth (cm)	Ca (%)	Mg(%)	K(%)	Na (%)	Zr (ppm)	Ti (%)
Asa	K1	80-90	1.41	0.51	0.93	1.06		0.34
	K4	80-90	1.29	0.44	0.88	1.00	288.1	-
	F3	60-70	1.41	0.55	0.87	1.04	282.6	-
	F4	80-90	1.26	0.49	0.85	0.98	293.3	-
Flakaliden	10B	60-70	1.09	0.57	0.88	0.87	243.8	-
	14B	60-70	1.59	0.70	0.81	1.03	336.1	-

1069  
1070



1071  
1072

**Table 4a.** Site parameters used in the PROFILE model

Parameter	Source	Asa	Flakaliden
Temperature (°C)	Measurements at Asa and Flakaliden	6.1	2.3
Precipitation (m yr <sup>-1</sup> )	Measurements at Asa and Flakaliden	0.736	0.642
Total deposition (mmol <sub>c</sub> m <sup>-2</sup> yr <sup>-1</sup> )	Measured data on open field and throughfall deposition available from nearby Swedish ICP Integrated Monitoring Sites	SO <sup>2-4</sup> : 27.0 Cl <sup>-</sup> : 38.3 NO <sup>3</sup> : 30.7 NH <sup>4</sup> : 21.6 Ca <sup>2+</sup> : 7.2 Mg <sup>2+</sup> : 6.8 K <sup>+</sup> : 1.9 Na <sup>+</sup> : 31.5	SO <sup>2-4</sup> : 13.1 Cl <sup>-</sup> : 5.6 NO <sup>3</sup> : 10.5 NH <sup>4</sup> : 9.9 Ca <sup>2+</sup> : 5.2 Mg <sup>2+</sup> : 1.9 K <sup>+</sup> : 1.1 Na <sup>+</sup> : 5.6
Base cation net uptake (mmol <sub>c</sub> m <sup>-2</sup> yr <sup>-1</sup> )	Previously measured data for Asa and Flakaliden: Concentrations in biomass from Linder (unpublished data). Biomass data from Heureka simulations.	Ca <sup>2+</sup> : 46.2 Mg <sup>2+</sup> : 10.6 K <sup>+</sup> : 17.8	Ca <sup>2+</sup> : 26.7 Mg <sup>2+</sup> : 4.4 K <sup>+</sup> : 6.7
Net nitrogen uptake (mmol <sub>c</sub> m <sup>-2</sup> yr <sup>-1</sup> )	Previously measured data from Asa and Flakaliden: Concentrations in biomass from Linder (unpublished data). Biomass data from Heureka simulations.	81.0	32.4
Base cations in litterfall (mmol <sub>c</sub> m <sup>-2</sup> yr <sup>-1</sup> )	Literature data from Hellsten et al. (2013)	Ca <sup>2+</sup> : 116.8 Mg <sup>2+</sup> : 15.1 K <sup>+</sup> : 10.5	Ca <sup>2+</sup> : 40.6 Mg <sup>2+</sup> : 4.6 K <sup>+</sup> : 3.2
Nitrogen in litterfall (mmol <sub>c</sub> m <sup>-2</sup> yr <sup>-1</sup> )	Literature data from Hellsten et al. (2013)	179.8	47.5
Evapo-transpiration (Fraction)	Precipitation data and runoff data. Runoff data calculated based on proportion of runoff to precipitation (R/P) at Gammtratten and Aneboda.	0.3	0.6

1073

1074

1075 **Table 4b.** Soil\* parameters used in the PROFILE model.  
 1076

Parameter	Unit	Source
Exposed mineral surface area	$\text{m}^2 \text{m}^{-3}$	Own measurements used together with Eq. 5.13 in Warfvinge and Sverdrup (1995)
Soil bulk density	$\text{kg m}^{-3}$	Own measurements
Soil moisture	$\text{m}^3 \text{m}^{-3}$	Based on paragraph 5.9.5 in Warfvinge and Sverdrup (1995)
Mineral composition	Weight fraction	Own measurements
Dissolved organic carbon	$\text{mg L}^{-1}$	Previously measured data for Asa and Flakaliden: Measurements for B-horizon from Harald Grip and previously measured data from Fröberg et al. (2013)
Aluminium solubility coefficient	$\text{kmol m}^{-3}$	Own measurements for total organic carbon and oxalate-extractable Al together with function developed from previously published data (Simonsson and Berggren, 1998)
Soil solution $\text{CO}_2$ partial pressure	atm.	Based on paragraph 5.10.2 in Warfvinge and Sverdrup (1995)

1077 \*) Physical and chemical soil horizon specific input data are given in supplements (Tables S3)  
 1078

1079  
1080

**Table 5.** Judgement of data quality for terms included in the base cation budget estimate of weathering.

Term	Spatial scale	Temporal scale	Data source	Quality of term quantification
Deposition	Adjacent sites	Annual or monthly measurements	Svartberget experimental forest, and Integrated Monitoring site	Moderate: high quality of data, but estimates are not site-specific
Soil stock change	Site (initial) and plot (repeated)	Repeated samplings (2)	J. Bergholm and H. Grip, unpublished data.	Moderate/low: repeated sampling biased by differences in methods of sampling and soil extraction.
Leaching	Plot	Sampling of soil water at 50 cm depth repeated 2 times per year. Water flux modelled (COUP).	H. Grip, unpublished data	High/moderate: High spatial and temporal resolution in soil chemistry, but uncertainty in separating lateral and vertical flow (Flakaliden).
Biomass accumulation	Site (control plots)	Growth increment measured from biomass studies at start and after 12 years.	Growth Albaugh et al. (2009) Nutrient content: S: Linder unpublished data	High/moderate: High quality in growth estimates and nutrient content at treatment scale, data lacking at plot scale

1081

1082

1083 **Table 6:** Standard errors and standard uncertainties ( $\text{mmol}_c \text{m}^{-2} \text{yr}^{-1}$ ) for the terms in the base cation budget,  
 1084 Eq. (4). Combined standard uncertainty, plot average value and confidence interval for the weathering rate of  
 1085 base cation  $i$  derived from base cation budgets  $W_{\text{budget}, i}$  ( $\text{mmol}_c \text{m}^{-2} \text{yr}^{-1}$ ).  
 1086

Site	Element	Deposition	Soil change	Biomass accum.	Leaching	Combined standard uncertainty	$W_{\text{budget}}$	Confidence interval (combined standard uncertainty $\times 3$ )
Asa	Ca	1.1	12.9	19.5	3.2	24	58	$\pm 71$
	Mg	1.1	0.6	2.5	1.6	3	29	$\pm 10$
	K	0.3	1.0	9.7	0.1	10	37	$\pm 29$
	Na	4.0	0.9	0.0	5.1	7	7	$\pm 20$
Flakaliden	Ca	0.8	10.5	13.3	0.7	17	28	$\pm 51$
	Mg	0.3	1.1	1.5	0.3	2	12	$\pm 6$
	K	0.2	0.6	6.7	0.2	7	19	$\pm 20$
	Na	0.7	1.2	0.0	0.8	2	2	$\pm 5$

1087  
 1088

1089 **Figure captions**

1090 **Figure 1.** Map of Scandinavia showing the location of the study sites Asa and Flakaliden.

1091

1092 **Figure 2.** Zirconium (Zr) gradient in the soil at Asa (K1, K4, F3, F4) and Flakaliden (10B, 11B, 14B, 15A).

1093

1094 **Figure 3.** (Left) Historical weathering rate of base cations ( $\text{mmolc m}^{-2} \text{yr}^{-1}$ ) estimated by the depletion method  
1095 and (right) steady-state weathering rate estimated by the PROFILE model in different soil layers at Asa and  
1096 Flakaliden.

1097

1098 **Figure 5.** Site mean values and standard errors (SE) of weathering rates ( $\text{mmolc m}^{-2} \text{yr}^{-1}$ ) for Ca, Mg, K and Na  
1099 determined with the depletion method, the PROFILE model and the base cation budget method for the 0-50 cm  
1100 horizon at Asa and Flakaliden. For the weathering rates based on the depletion method and the PROFILE model,  
1101 error bars represent the SE calculated based on four soil profiles at each study site, except for Flakaliden, where  
1102 the depletion method was only applied in two soil profiles. For weathering rates based on the base cation  
1103 budget approach, SE bars were calculated from combined standard uncertainties, which are based on SE derived  
1104 from plot-wise replicated data of the present experiments (for leaching and changes in exchangeable soil pools)  
1105 and on standard uncertainties derived from Simonsson et al. (2015), where replicated data were missing in the  
1106 present study (for accumulation in biomass and total deposition).

1107

1108 **Figure 6.** (Left) Sinks and (right) sources of base cations (BC) in ecosystem net fluxes at Asa and Flakaliden.  
1109 The soil is a net source of soil BC if soil base cation stocks decrease and a net sink if they increase. 'BC budget'  
1110 = current base cation weathering rate ( $W_{\text{budget}}$ ) estimated with the BC budget method, including measured  
1111 changes in soil exchangeable BC stocks; 'PROFILE'= soil exchangeable pools estimated from BC budget using  
1112 PROFILE estimates of BC weathering rate; 'Historical'=soil exchangeable pools estimated from BC budget  
1113 using estimates of historical weathering rate by the depletion method. 'Measured soil change' and 'Base cation  
1114 budget estimated soil change' indicates that equation 4 was used to estimate weathering rate, or the soil change,  
1115 respectively.

1116

1117 **Figure 7.** Time (years) required to achieve the measured historical element loss in different soil horizons with  
1118 application of maximum or minimum PROFILE weathering rates at (a) Flakaliden and (b) Asa.

1119

1120



1121

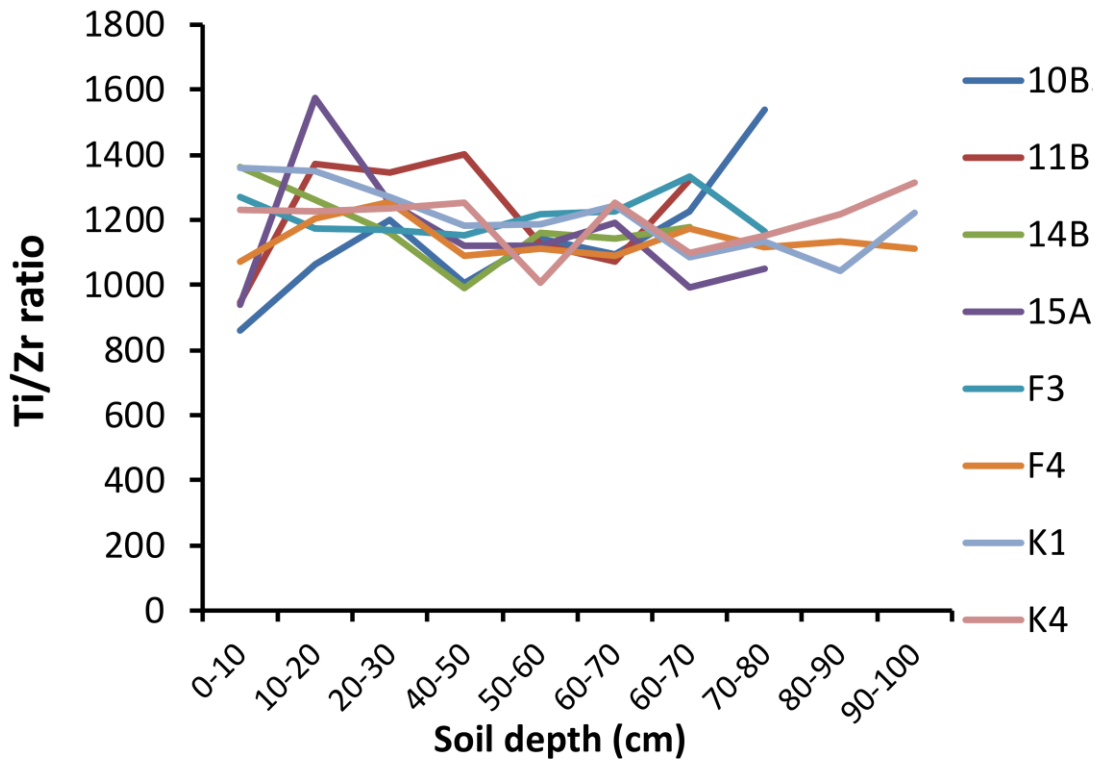
1122

1123

1124

**Figure 1.**

1125



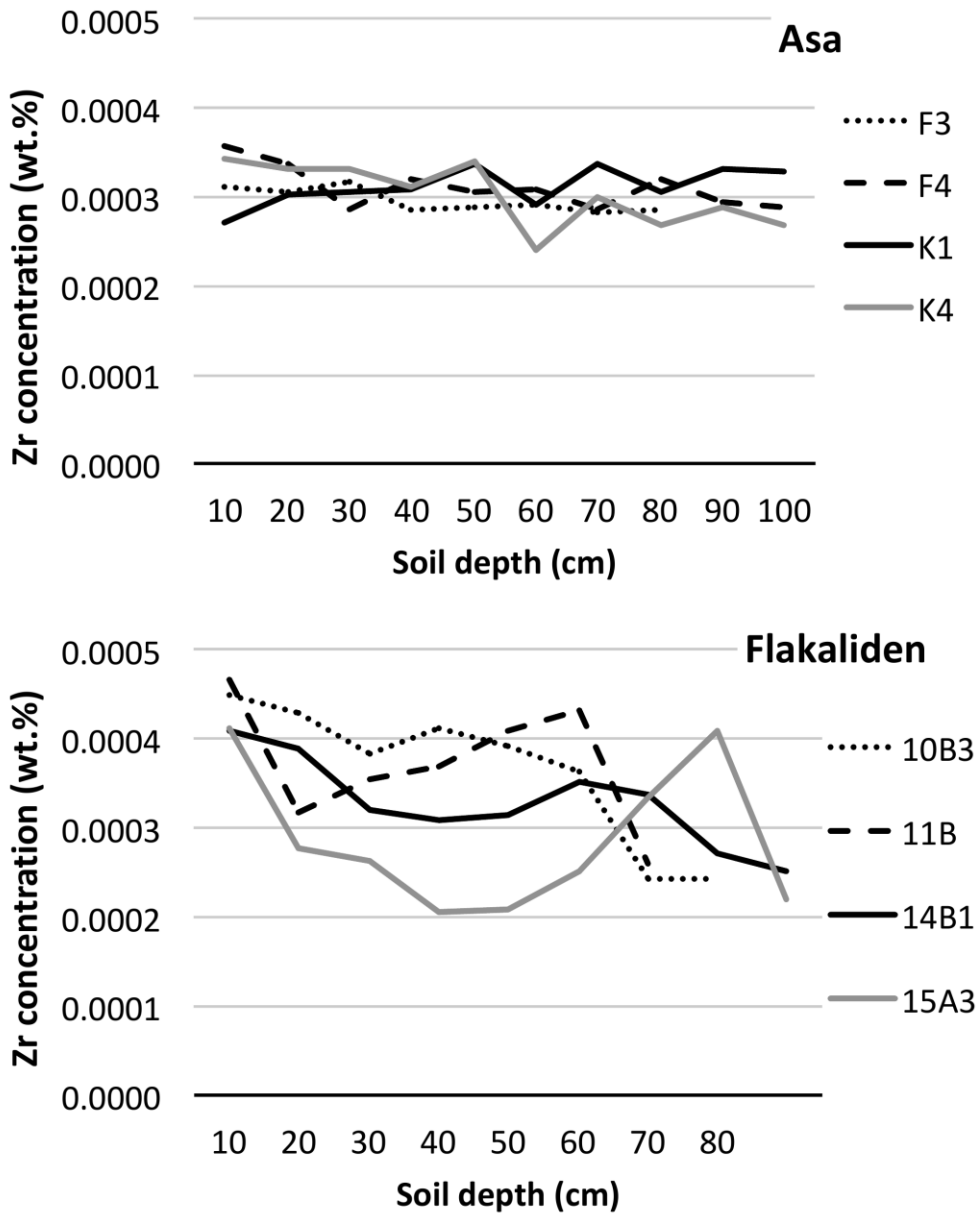
1126

1127

1128 Figure 2.

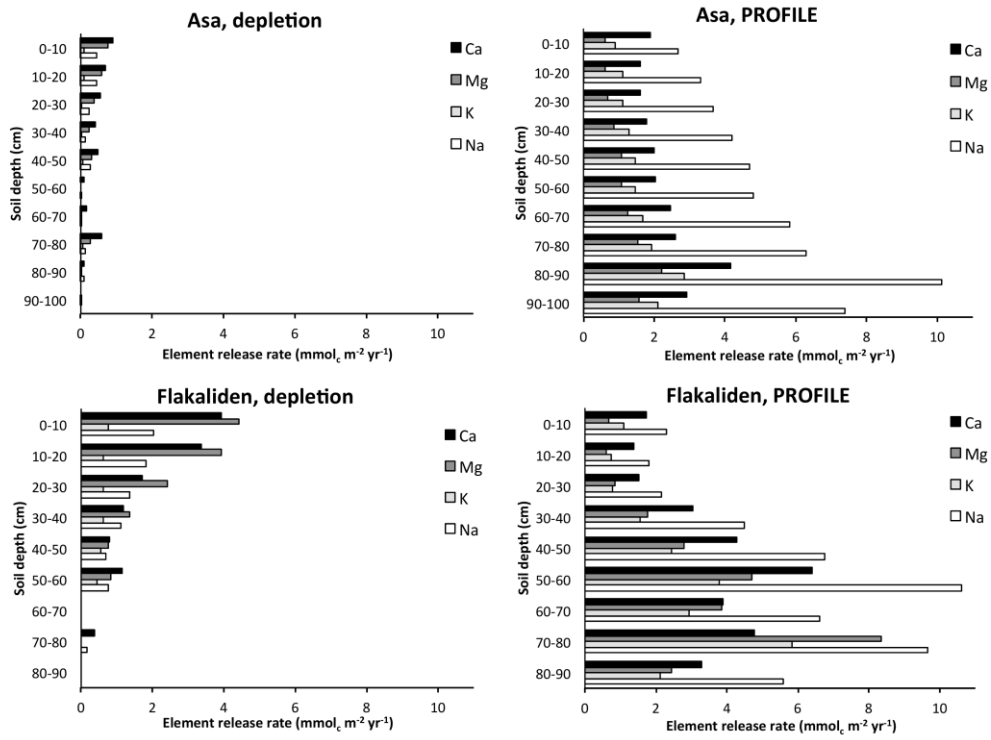
1129

1130



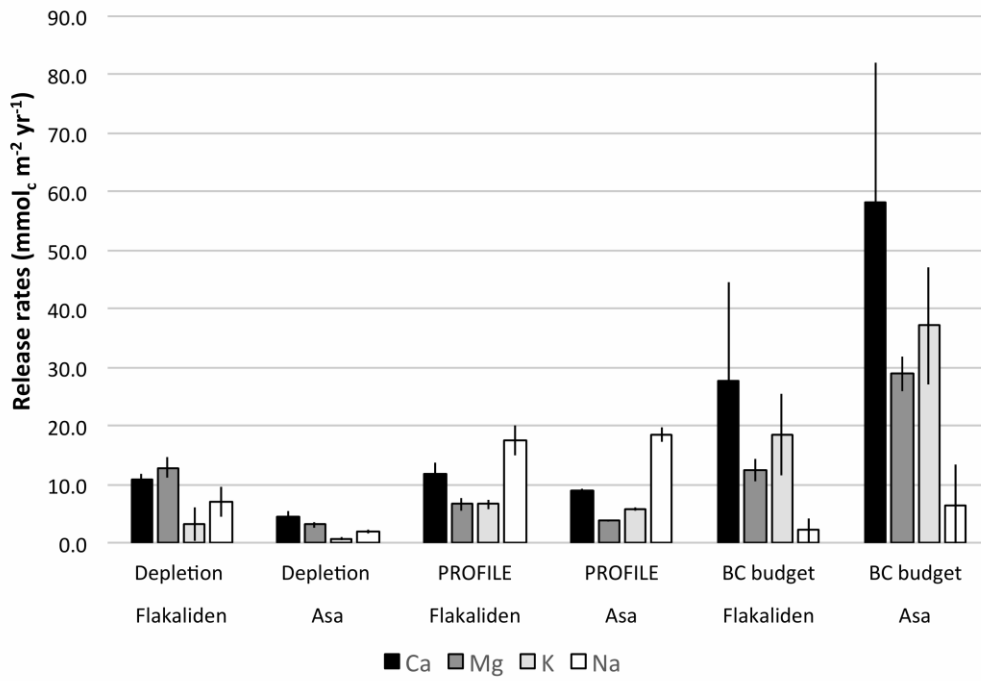
1131  
 1132  
 1133 Figure 3  
 1134



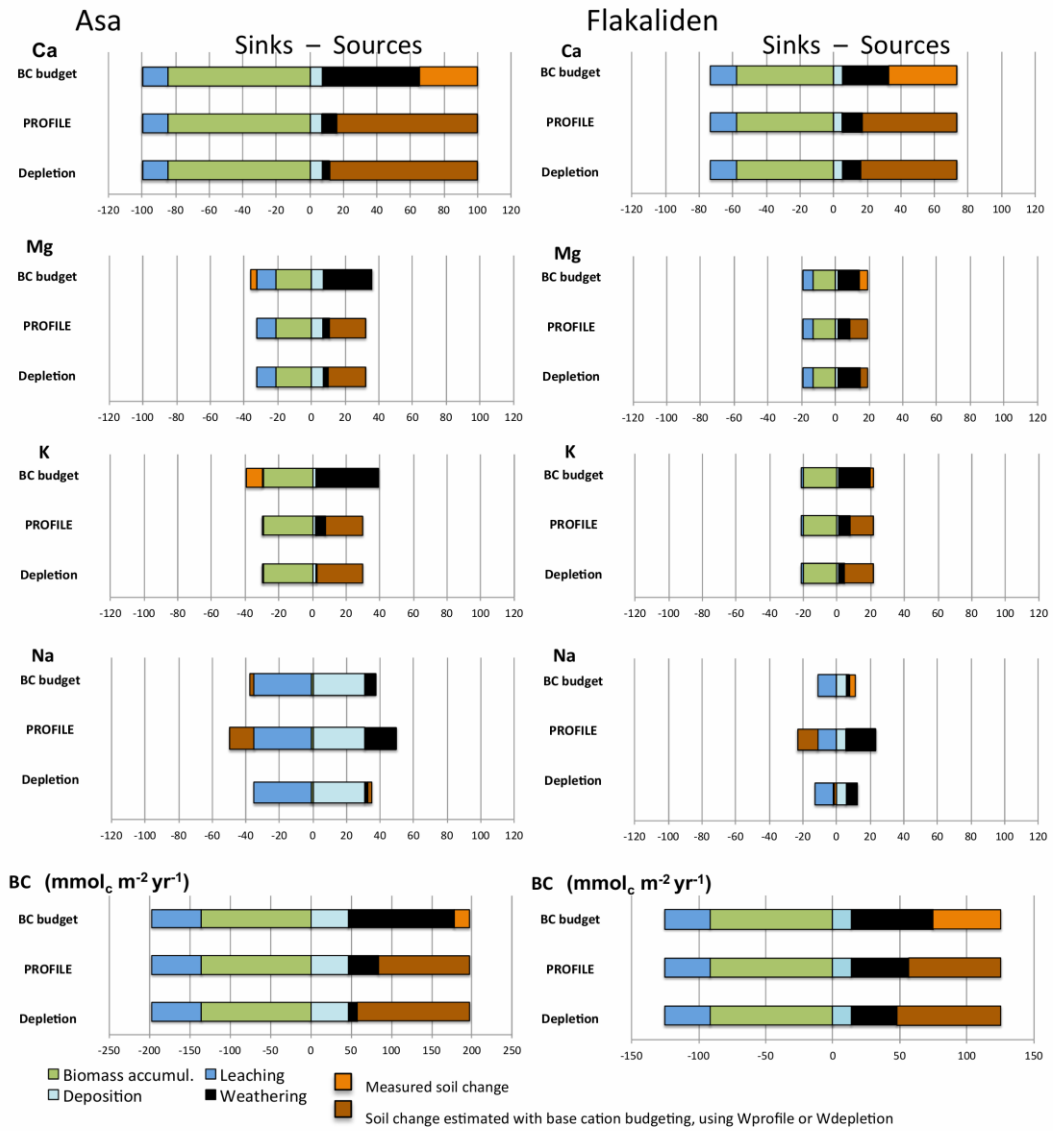


1135  
 1136  
 1137  
 1138  
 1139

Figure 4.

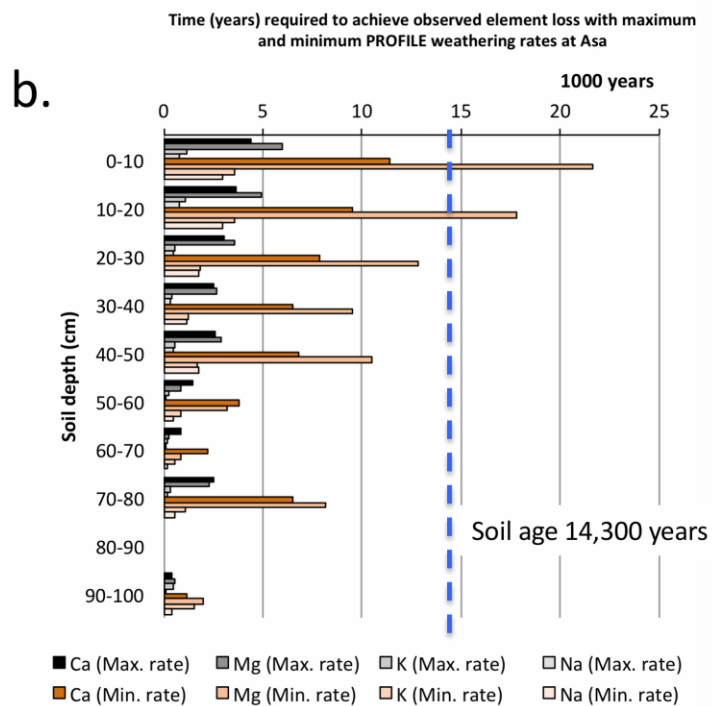
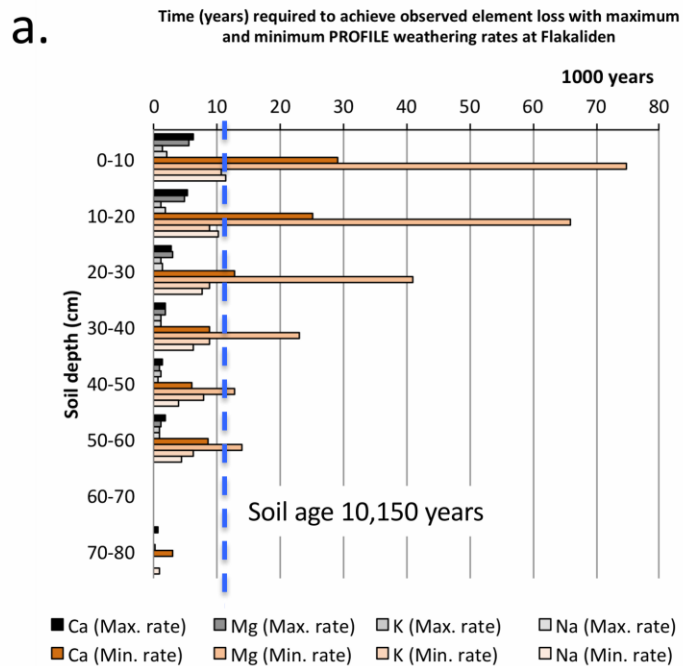


1140  
 1141 Figure 5.  
 1142  
 1143



1144  
 1145  
 1146  
 1147

Figure 6.



1148  
1149  
1150

Figure 7.